IEEE Access
Multidisciplinary | Rapid Review | Open Access Journal

Received February 8, 2020, accepted February 24, 2020, date of publication February 27, 2020, date of current version March 10, 2020.

Digital Object Identifier 10.1109/ACCESS.2020.2976774

A Loop Pairing Method for Non-Linear Multivariable Control Systems Under a Multi-Objective Optimization Approach

VÍCTOR HUILCAPI[1], XAVIER BLASCO[2], JUAN MANUEL HERRERO[2], AND GILBERTO REYNOSO-MEZA[3]

[1]Facultad de Ingenierías, Universidad Politécnica Salesiana, Guayaquil 09014752, Ecuador
[2]Instituto Universitario de Automática e Informática Industrial, Universitat Politècnica de València, 46022 Valencia, Spain
[3]Programa de Pós-Graduação em Engenharia de Produção e Sistemas (PPGEPS), Pontifícia Universidade Católica do Paraná (PUCPR), Curitiba 80215-901, Brazil

Corresponding author: Víctor Huilcapi (vhuilcapi@ups.edu.ec)

This work was supported in part by the Ministerio de Ciencia, Innovación y Universidades, Spain, under Grant RTI2018-096904-B-I00, in part by the Direcció General de Ciència i Investigació, Generalitat Valenciana, Spain, under Grant AICO/2019/055, in part by the Conselho Nacional de Pesquisa e Desenvolvimento (CNPq), in part the Fundação Araucária (FAPPR) - Brazil under Grant 304066/2016-8-PQ2, Grant 437105/2018-0-Univ, and Grant PRONEX-042/2018, and in part by the Universidad Politècnica Salesiana, Ecuador, under Grant CB-755-2015.

ABSTRACT In the multivariable control literature there are few techniques that face the problem of selecting suitable loop pairings in non-linear multivariable systems. Most techniques analyze the linearized system at a specific operating point. This paper proposes a new methodology to optimally and simultaneously select the loop pairings and the tuning of the parameters of the decentralized control by applying a multi-objective optimization approach directly on the non-linear system. The main contribution of this work is that the proposed methodology enables a detailed multi-dimensional analysis of the performances and trade-offs in the available loop pairings to control a multivariable non-linear system. The methodology is applied in this paper to three examples that analyze how the different types of loop pairings conflict. In one of the examples, the proposed methodology was applied first in the linearized system and later in the non-linear system. The results were contradictory and show how the application of loop pairing techniques for linear systems can be inaccurate when they are applied on a non-linear system previously linearized at an operating point. The following examples show that the operating point of a non-linear system, the design objectives of each multi-objective problem, as well as the designer's preferences have important roles in the selection of an optimal loop pairing.

INDEX TERMS Multivariable control system, non-linear systems, loop pairing, decentralized control structures, multi-objective evolutionary optimization, Pareto front.

I. INTRODUCTION

The development of efficient control strategies for multiple-input and multiple-output (MIMO) systems remains a challenge for designers or control engineers. This challenge is due to the complexity of the multiple interactions that exist between all the variables in a MIMO system.

In the field of multivariable control research there are two major approaches to control this type of system: centralized control or decentralized control. Each approach has advantages and disadvantages for the control of multivariable systems. In a decentralized control approach, the main benefits are: ease of implementation; existence of simple procedures for tuning controllers; and effectiveness for maintaining control loops (open control loops without the entire plant remaining off-line) [1]–[4].

Centralized control approaches consist of a single controller that has a global vision of the multivariable system and the interactions between all the variables. An important example of this type of controller is known as Model Predictive Control (MPC). The main advantage of a centralized control, compared to a decentralized one, is that it calculates control actions considering all the interactions of the MIMO system. Among the advantages of the MPC, it is worth mentioning the following ones: 1) it uses a process model to obtain predictions of the dynamic evolution; 2) it uses also the concept of

The associate editor coordinating the review of this manuscript and approving it for publication was Mauro Gaggero.

moving horizon, which allows to recalculate control actions when new process measures are available; 3) it can naturally compensate the dead times that exist in a wide variety of industrial processes as well as measurable disturbances. One of the main limitation of the MPC is that its performance depends on the model accuracy. Another disadvantage is its high computational cost, as MPC generally requires to solve an optimization problem in real time. This aspect is becoming less and less problematic due to the advance of computer systems [5], [6].

It is important to mention that to perform an efficient decentralized control of a multivariable system it is necessary to make an adequate selection of input-output pairings. The selection of loop pairings to control a MIMO system is not a simple task (for example, in an $n \times n$ system there are $n!$ possible loop pairings available to control the system). A seminal work on loop pairing methodology for linearized and time-invariant MIMO systems established the relative gain array (RGA) [7]. After Bristol's work, important contributions were made with new methodologies for the selection of loop pairings with a focus on linearized systems (e.g., [8]–[11]).

Among the contributions to face the problem of selecting suitable input-output pairings for the decentralized control of a non-linear MIMO system is the *relative-order matrix* proposed in [12]. The relative order matrix was initially used as an overview of the interaction between the input-output of a non-linear MIMO system. An *initial extension of RGA* that quantified the interactions between the input-output of a non-linear MIMO system was proposed in [13], and later the *non-linear relative gain array (NRGA)* was defined in [14], [15].

It is important to mention that when a multivariable system is linearized at an operating point, the RGA, as well as the relative-order matrix or the NRGA for the same operating point, can provide different information on the type of input-output pairing to choose. This shows that the task of selecting loop pairings to control a multivariable non-linear system is complex due to the characteristics of these systems [16].

Another relevant aspect to achieve an efficient decentralized control of a non-linear multivariable system is the tuning of the system controllers. It is possible to successfully tune the control structures of a non-linear MIMO system by applying an optimal design.

Metaheuristics are non-deterministic techniques that simulate the behavior of some kind of natural phenomenon or system to solve optimization problems. They have demonstrated good performance in solving complex problems (difficult to address by traditional mathematical methods), both in benchmark and real-life problems [17], [18].

Metaheuristics can be classified into two groups: those that are nature-inspired and those that are not. Important examples of nature-inspired metaheuristics are evolutionary algorithms (EA) and algorithms using swarm intelligence. Genetic algorithms (GA) can be considered as one of the most representative methods of EA [19], [20].

Particle swarm optimization algorithms (PSO) are based on the intelligent behavior of social insect colonies (bees, ants, fireflies, butterflies, among others). [21]–[23]. Among the most recent swarm metaheuristics is the Seeker optimization algorithm, which is based on human group search behavior. [24], [25]. EAs have been successfully hybridized with the swarm intelligence approach [26]–[28].

Gradually, evolutionary techniques have been used and further developed to solve multi-objective optimization problems. A significant example is the multi-objective evolutionary algorithms (MOEA), which have been successfully applied to many real engineering problems. MOEAs are flexible enough to handle non-convex functions with hard restrictions and high non-linearity [29]–[33]. For this reason, a MOEA has been chosen for solving the multi-objective optimization problems that arise in the tuning of the control structures of the non-linear systems analyzed in this work.

A MOEA finds a satisfactory approximation of the Pareto front of a multi-objective problem (MOP) and in the decision-making stage a designer can select an optimal solution according to his or her preferences. There are several tools designed to help designers to select optimal Pareto front solutions as briefly summarized in [34], [35].

Visualization tools have proven powerful in the decision-making stage and have been widely accepted for helping designers to choose optimal Pareto solutions [36]–[38]. When the dimension of a MOP is increased, the decision making task becomes more complex and alternative visualization tools are required (some examples are, among others: Level diagrams, Scatter diagrams, Parallel coordinates and Star diagrams) [39], [40].

The level diagrams (LD) tool has interesting features to help the designer easily interpret and choose solutions from a Pareto front. The main features of LD include: flexibility to incorporate different design points of view (with different types of synchronization norms); ability to compare different design concepts; highlighting and coloring solutions; and multi-dimensional interactivity between fronts [41], [42].

In the multi-objective optimization process, the *ev*-MOGA algorithm[1] was used to find the Pareto fronts [43]–[45]. However, it is important to emphasize that the methodology proposed in this work can be applied with different optimization algorithms, since it is independent of the optimization algorithm used, as long as it guarantees a satisfactory quality level.

The level diagrams (LD) tool[2] was used to perform the m-dimensional analysis of each Pareto front. To compare the different design concepts proposed in this paper, the Pareto front quality indicator *QI* proposed in [50] was applied.

[1] *ev*-MOGA algorithm available at: https://es.mathworks.com/matlabcentral/fileexchange/31080-ev-moga-multiobjective-evolutionary-algorithm.

[2] Level diagrams interactive tool available at: https://es.mathworks.com/matlabcentral/fileexchange/62224-interactive-tool-for-decision-making-in-multiobjective-optimization-with-level-diagrams.

LD and QI enable global evaluation of the Pareto fronts of each MOP by applying Pareto dominance analysis.

This paper aims to contribute to the generation of a framework that enables extending the multi-objective methodology proposed in [46] to design decentralized controllers (loop pairing and optimal tuning of controller parameters) in non-linear multivariable systems. It is important to mention that according to [46] and [47] the selection of an optimal loop pairing depends on the designer's preferences regarding the design objectives of the multi-objective problem (MOP) and the satisfactory tuning of the system controllers. An interesting aspect of the proposed loop pairing methodology is that it is associated with both the selection of input-output pairings, as well as the tuning of each MIMO system controller in the multi-objective optimization (MOO) process.

This new methodology is compared to other methodologies from the existing literature and its benefits and convenience are demonstrated.

For this purpose, the proposed multi-objective loop pairing methodology is applied to three examples using two non-linear multivariable systems. In the first example, a coupled two-tank process like the one shown in [48] is analyzed, and a control valve is added to generate a 2×2 MIMO system. In the second and third examples, the quadruple-tank process (4×4 MIMO system) proposed in [49] is analyzed.

To explore the input-output pairings of the coupled two-tank process, the system was linearized at an operating point and the methodology presented in [46] was applied. The performance of each loop pairing and the optimal tuning of the system controllers were determined. Subsequently, the methodology proposed in this paper was applied directly to the non-linear system under the same operating conditions and a different scenario was revealed (compared to that obtained for the linearized system). This shows that the results obtained on the linearized system (loop pairing) do not necessarily have to coincide with the non-linear system. Therefore, we propose to extend the methodology shown in [46] and directly apply it to non-linear multivariable systems. The results obtained for the non-linear system of coupled two-tanks were satisfactory. The behavior of the system in a different operating area was analyzed and it was revealed how loop pairings for a non-linear system can be affected by the operating point (depending on the operating point). Finally, a system analysis scenario with a greater number of design objectives for each MOP was proposed and it was revealed how a designer's preferences over these objectives can affect the choice of a loop pairing to control a non-linear multivariable system.

In the second example, the methodology proposed in this paper was applied to the quadruple-tank process proposed by [49]. The system was analyzed when it presents non-minimum phase dynamics and the levels of the lower tanks of the system are controlled with the available pumps. In this example, MOPs with four design objectives are proposed to analyze the reference tracking error of each output and the control efforts of each input independently. This example reveals that loop pairings to control this non-linear system are in conflict, and that an input-output pairing is better for controlling a system output and vice versa. Also with the proposed methodology, it was feasible to tune controllers with better performances than those proposed in [49].

Finally, as a third example, the input-output pairings to control all levels of the system tanks (quadruple-tank process) using all available pumps and valves are analyzed. In this example, MOPs with eight design objectives are proposed to evaluate the reference tracking error of each output and the control effort of each input independently. It is possible to find a loop pairing that successfully controls the level of each tank. This last example is proposed to show the applicability of the methodology in non-linear MIMO systems with a greater number of inputs and outputs. The increase in system inputs and outputs also increases the number of input-output pairings and the computational cost of the methodology.

Through the examples shown in this paper, the applicability of the extension of the methodology proposed in [46] for non-linear multivariable systems is demonstrated. The proper selection of an input-output pairing to perform the decentralized control of a non-linear MIMO system is strongly related to the following aspects: the designer's preferences over the design objectives of each MOP; the optimal tuning of control structures; as well as the operation zone where a non-linear multivariable system is analyzed. The ability of the proposed multi-objective methodology to offer to the control engineer a multi-dimensional approach to solving loop pairing problems is also demonstrated.

This paper is structured as follows: Section II shows the basics of multi-objective optimization and a brief introduction about what is described in this paper as a design concept. Section III shows the extension of the multi-objective proposal of loop pairing for application in non-linear multivariable systems. In Sections IV, V and VI the proposed methodology is applied to the non-linear multivariable systems mentioned previously. Finally, some conclusions are presented in Section VII.

II. BACKGROUND OF MULTI-OBJECTIVE OPTIMIZATION

When a control engineer solves problems where there are conflicting objectives (that is, improving some objectives worsens others) it is advisable to perform a multi-dimensional analysis and apply multi-objective optimization techniques.

A multi-objective optimization problem (MOP) can be defined as shown in (1)-(5).

$$\min_{\mathbf{x}} \mathbf{J}(\mathbf{x}) \tag{1}$$

$$\mathbf{J}(\mathbf{x}) = \{J_1(\mathbf{x}), J_2(\mathbf{x}), \ldots, J_s(\mathbf{x})\} \tag{2}$$

subject to:

$$g(\mathbf{x}) \leq 0 \tag{3}$$

$$h(\mathbf{x}) = 0 \tag{4}$$

$$\underline{\mathbf{x}} \leq \mathbf{x} \leq \overline{\mathbf{x}} \tag{5}$$

where $\mathbf{x} = (x_1, x_2, \ldots x_n) \in \mathbf{R}^n$ represents the decision vector; $\mathbf{J}(\mathbf{x}) \in \mathbf{R}^m$ represents the vector of design objectives;

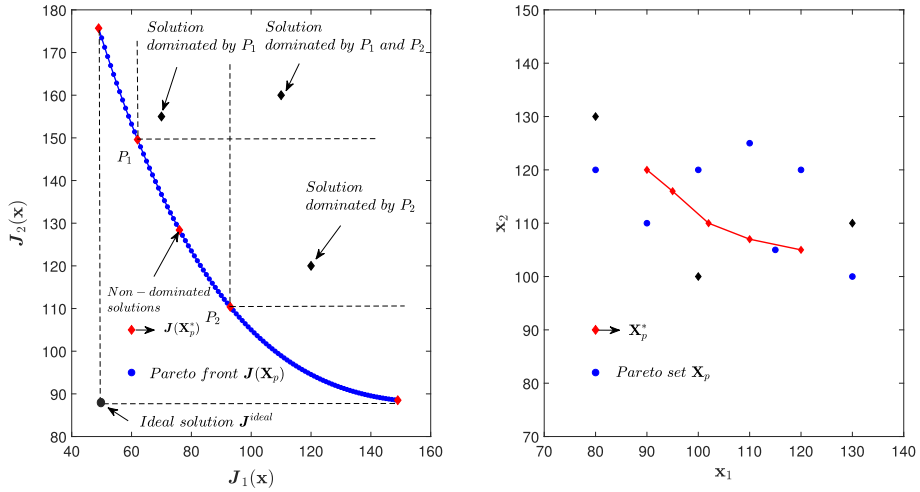

FIGURE 1. Pareto front, Pareto set, and basic notion of Pareto dominace.

$g(\mathbf{x})$, $h(\mathbf{x})$ are the constraints vectors; and $\underline{\mathbf{x}}, \overline{\mathbf{x}}$ are the lower and upper bounds of each dimension of the decision space.

The solution of a MOP is not unique, since there is a set of optimal solutions for each MOP. This set of optimal solutions is known as the Pareto front. On the Pareto front, each solution has a different level of compromise between the design objectives of the proposed MOP (that is, no solution is better than another) [51].

It is possible to build an optimal Pareto set $\mathbf{X}_p$ by applying a *Pareto dominance analysis* [52], [53] (see Fig. 1).

A Pareto dominance definition is shown in (6) and the optimal Pareto set $\mathbf{X}_p$ can be defined as in (7), and its corresponding Pareto front in (8).

$$\forall i \in \{1,\ldots,s\}, \quad \mathbf{J}_i(\mathbf{x}^1) \leq \mathbf{J}_i(\mathbf{x}^2) \ \wedge \ \exists k \in \{1,\ldots,s\} : \mathbf{J}_k(\mathbf{x}^1) < \mathbf{J}_k(\mathbf{x}^2) \tag{6}$$

$$\mathbf{X}_p = \{\mathbf{x} \in D | \ \nexists \mathbf{x}' \in D : \mathbf{x}' \leq \mathbf{x}\} \tag{7}$$

$$\mathbf{J}(\mathbf{X}_p) = \{\mathbf{J}(\mathbf{x}) | \mathbf{x} \in \mathbf{X}_p\} \tag{8}$$

It is important to consider that in practical engineering problems the Pareto front is generally unknown and the MOEAs find a solutions set $\mathbf{X}_p^*$ that is a subset of $\mathbf{X}_p$, where $\mathbf{J}(\mathbf{X}_p^*)$ satisfactorily approximates $\mathbf{J}(\mathbf{X}_p)$.

Once the Pareto front is obtained, it is possible to select solutions according to preferences that a designer has for solving a MOP. For example, a designer's preference might be to select the Pareto front solution closest to the ideal solution for the MOP (see Fig. 1). Another preference could be to select solutions in a specific zone of interest of the Pareto front as shown in Fig. 2 (a).

To compare different Pareto fronts in this paper (corresponding to different design concepts) and analyze their performance, the LD tool with different synchronization norms was used as shown in [46], [50]. Fig. 2 compares two Pareto fronts associated with two design concepts (each concept proposes a MOP with two objectives), where there are four zones with different characteristics. Zone 1 is covered only by the design concept B. In zone 2, the design concept B dominates design concept A, and the $QI - norm$ of concept B is less than one ($QI < 1$) as shown in Fig. 2(c). The opposite occurs in zone 3 (concept A dominates concept B) and finally zone 4 is covered only by design concept A. The LD tool allows a designer to select solutions synchronously in each design concept according to his or her preferences as shown in Fig. 2 (b), (c) (solutions highlighted in yellow).

III. MULTI-OBJECTIVE PROPOSAL FOR THE SELECTION OF INPUT-OUTPUT PAIRINGS IN NON-LINEAR MULTIVARIABLE SYSTEMS

Consider a multivariable non-linear system to be controlled with n inputs $(u_1,\ldots,u_n)$ and n outputs $(y_1,\ldots,y_n)$ defined by (9).

$$\begin{aligned} \dot{x} &= f(x,u) \\ y &= h(x,u) \end{aligned} \tag{9}$$

where the *state vector* $x = (\mathsf{x}_1, \mathsf{x}_2, \ldots, \mathsf{x}_m) \in \mathbf{R}^m$, $u_i, y_i \in \mathbf{R}^n$. The multivariable decentralized control for the non-linear MIMO system[3] described in (9) (for some generic operating point $\wp$ or system operation zone) is defined by: 1) a vector $\mathbf{c}_k$ whose elements represent the controllers to stabilize the system outputs as shown in (10); and 2) an input-output pairing matrix $L_p^{c_k}$ that connects the outputs $\hat{u}_i$ of each controller with the inputs u_i of the non-linear MIMO system as shown in (11).

$$\mathbf{c}_k = \left[C^{c_k}_{y_1,\hat{u}_1}, \ldots C^{c_k}_{y_i,\hat{u}_i}, \ldots, C^{c_k}_{y_n,\hat{u}_n}\right] \tag{10}$$

$$\begin{bmatrix} u_1 \\ \vdots \\ u_i \\ \vdots \\ u_n \end{bmatrix} = L_p^{c_k} . \begin{bmatrix} \hat{u}_1 \\ \vdots \\ \hat{u}_i \\ \vdots \\ \hat{u}_n \end{bmatrix} \tag{11}$$

$$k \in \{1,\ldots,w\};$$

[3]The methodology is also valid for other ways of representing a non-linear system, and is applicable for any model that can be simulated.

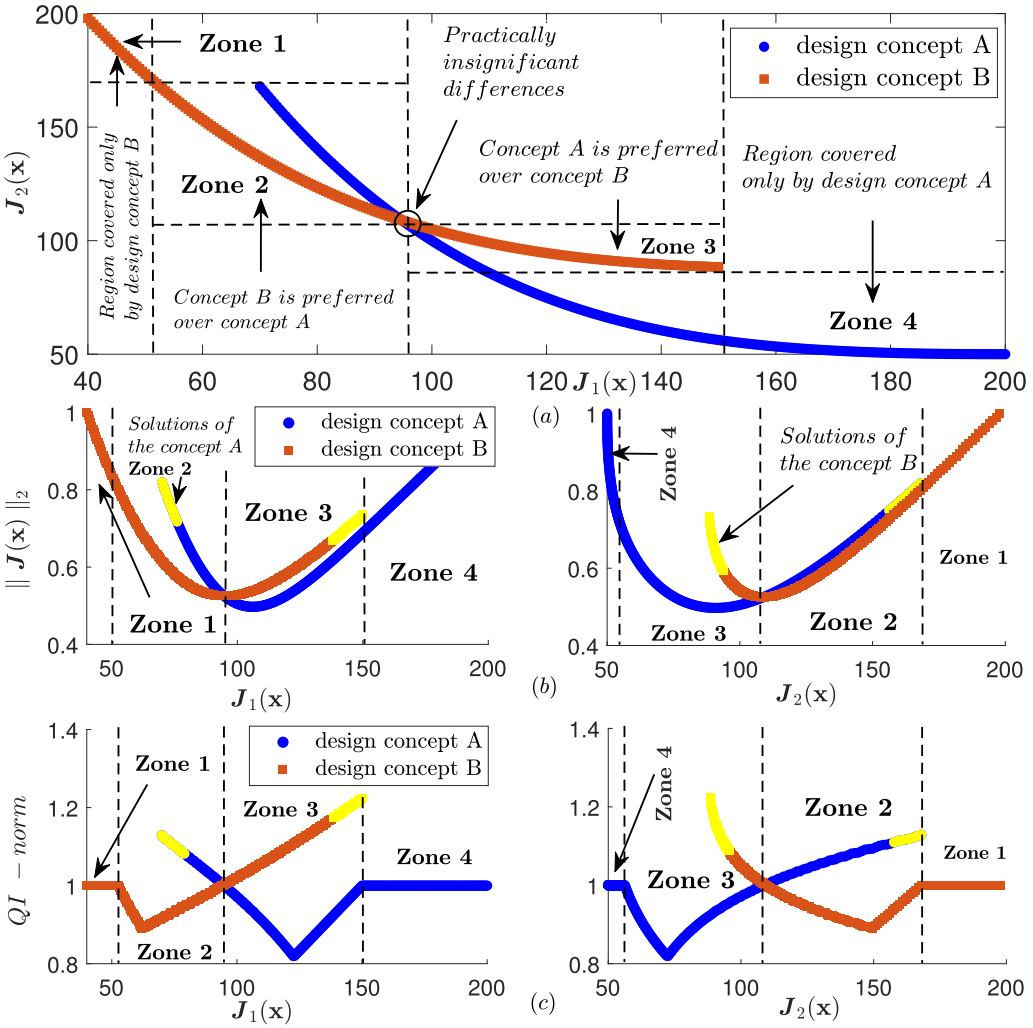

FIGURE 2. Pareto fronts and comparison of design concepts using *level diagrams* (LD). (a) Comparison of design concepts A and B in a bi-objective space. (b) Comparison of design concepts A and B using LD with 2-norm. (c) Comparison of design concepts A and B using LD with *QI*-norm.

In equation (10), $C^{c_k}_{y_i,\hat{u}_i}$ represents the controller that stabilizes the output y_i of the control $\mathbf{c}_k$. The controller $C^{c_k}_{y_i,\hat{u}_i}$ generates the control action $\hat{u}_i$ which is connected to an input u_i of the non-linear system using the loop pairing matrix $L_p^{c_k}$ as shown in Fig. 3. $L_p^{c_k}$ is a Boolean matrix $\mathfrak{B}_{nxn}$ as shown in (12).

$$L_p^{c_k} = \begin{bmatrix} l_{11} & \dots & l_{1n} \\ \vdots & \dots & \vdots \\ l_{n1} & \dots & l_{nn} \end{bmatrix}; \quad l_{ij} = 0, 1; \ \forall i, j = 1 \dots n \tag{12}$$

The matrix $L_p^{c_k}$ must have only logical value 1 in each row and column, since when adding all the elements of a row and/or column its result will be one. For example, for a non-linear system with four inputs and four outputs where y_1 is controlled with u_3 ($l_{31} = 1$), y_2 is controlled with u_4 ($l_{42} = 1$), y_3 is controlled with u_2 ($l_{23} = 1$), and y_4 is controlled with u_1 ($l_{14} = 1$). The matrix $L_p^{c_k}$ and the control efforts u_i are as shown in (13).

$$L_p^{c_k} = \begin{bmatrix} 0 & 0 & 0 & 1 \\ 0 & 0 & 1 & 0 \\ 1 & 0 & 0 & 0 \\ 0 & 1 & 0 & 0 \end{bmatrix} \Rightarrow \begin{bmatrix} u_1 \\ u_2 \\ u_3 \\ u_4 \end{bmatrix} = \begin{bmatrix} \hat{u}_4 \\ \hat{u}_3 \\ \hat{u}_1 \\ \hat{u}_2 \end{bmatrix} \tag{13}$$

Each controller $C^{c_k}_{y_i,\hat{u}_i}$ must also be tuned through a vector of setting parameters $\mathbf{x}^{ck}_{yi}$. The process control would therefore be parameterized by the vector shown in (14).

$$\mathbf{x}^{ck} = [\mathbf{x}^{ck}_{y1}, \dots, \mathbf{x}^{ck}_{yn}] \tag{14}$$

It is important to consider that in this proposed methodology, $\mathbf{c}_k$ refers to a design concept of the w design concepts that can be analyzed. Each design concept must be optimally tuned through its parameters $\mathbf{x}^{ck}$ by establishing a loop pairing $L_p^{c_k}$.

The proposed multi-objective optimization methodology generates for each design concept a set of optimal Pareto

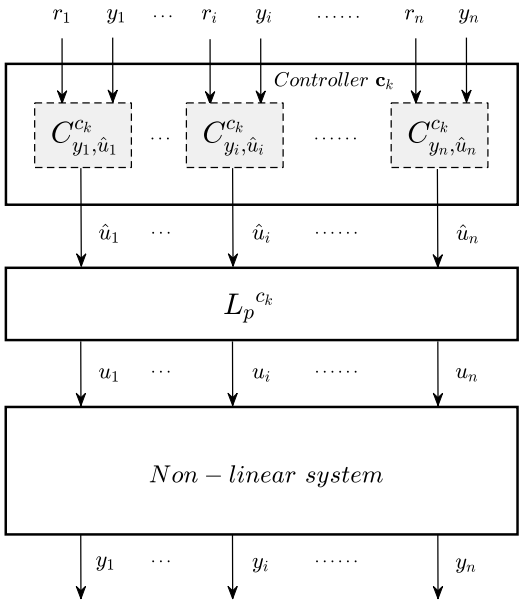

FIGURE 3. Block diagram of the decentralized non-linear multivariable control system defined in (10) and (11).

solutions $\mathbf{X}^{ck}$ and the corresponding Pareto front $\mathbf{J}(\mathbf{X}^{ck})$. Therefore, for each design concept, MOPs are proposed as shown in (15)-(17).

$$\mathbf{X}^{ck} = arg\min_{\mathbf{x}^{ck}} \mathbf{J}(\mathbf{x}^{ck}) \tag{15}$$

$$\mathbf{J}(\mathbf{x}^{ck}) = \left[J_1(\mathbf{x}^{ck}), \ldots, J_s(\mathbf{x}^{ck})\right] \tag{16}$$

$$\underline{\mathbf{x}}^{ck} \leq \mathbf{x}^{ck} \leq \overline{\mathbf{x}}^{ck} \tag{17}$$

where, $\underline{\mathbf{x}}^{ck}$ and $\overline{\mathbf{x}}^{ck}$ are the lower and upper bounds of the search space of the parameter vector $\mathbf{x}^{ck}$ for the concept $\mathbf{c}_k$. The design objectives $\mathbf{J}(\mathbf{x}^{ck})$ to be optimized are associated with each design concept $\mathbf{c}_k$ in the k MOPs.

The proposed methodology is shown in Fig. 4. In stage A, with the model of the non-linear MIMO system, it is possible to define a region where you want to control the system (operating points $\wp$). Thus, the analysis scenarios for each MOP must also be established by selecting the level of detail to analyze each loop pairing to control the system (it is possible to define scenarios with $2, 3, 4, \ldots, J_{i_{th}}(\mathbf{x}^{ck})$ design objectives). Subsequently, the design concepts (loop pairing and control structures) must be defined and the MOPs declared. Stage B is the multi-objective (MO) optimization stage where Pareto fronts (performance of each loop pairing) are obtained, as well as Pareto sets (controller parameters optimally adjusted). The Pareto fronts obtained in stage C for each MOP are evaluated and compared using the LD and QI tool. Finally, a designer or control engineer can choose, according to his or her preferences, an input-output pairing and the respective controllers that satisfactorily stabilize the non-linear MIMO system. If the results do not satisfy a designer, or if he/she wants to control the non-linear system in another system operation zone, the process can be repeated.

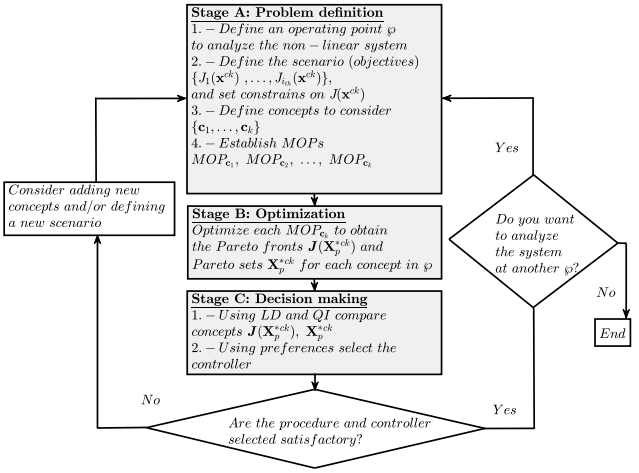

FIGURE 4. Flow chart of the proposed methodology for selecting pairings in non-linear multivariable systems.

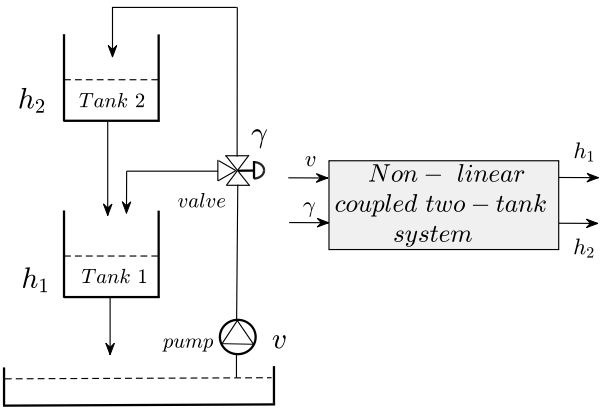

FIGURE 5. Schematic diagram of the coupled two-tank system.

IV. EXAMPLE 1: NON-LINEAR COUPLED TWO-TANK SYSTEM

The schematic diagram of the non-linear system of coupled two-tanks is shown in Fig. 5 and its first principles model is shown in (18), (19).

$$A_1 \frac{dh_1}{dt} = -a_1\sqrt{2gh_1} + a_2\sqrt{2gh_2} + \gamma kv \tag{18}$$

$$A_2 \frac{dh_2}{dt} = -a_2\sqrt{2gh_2} + (1-\gamma)kv \tag{19}$$

where:

A_1, A_2: cross-section of tanks 1 and 2.
a_1, a_2: cross-section of the outlet holes.
h_1, h_2: water levels.
γ: valve opening/closing coefficient.
v: voltage applied to the pump v.
k: coefficient of water inflow of pump v.
g: acceleration of gravity.

The system actuators present the constraints given by (20).

$$0 \leq v \leq 7.2\,V, \quad 0 \leq \gamma \leq 1 \tag{20}$$

TABLE 1. Parameters for the coupled two-tank system.

Parameter	Value
A_1	28 cm^2
A_2	32 cm^2
a_1	0.071 cm^2
a_2	0.057 cm^2
k	3.33 $cm^3/V.s$
g	981 cm/s^2

The parameters of the proposed model in (18), (19) are shown in Table 1.

This first example shows three important aspects to consider when selecting loop pairings in a non-linear system. These aspects are: a) the validity of a loop pairing on a linearized system does not guarantee a correct loop pairing in the non-linear system; b) the validity of a loop pairing for different operating points of a non-linear multivariable system; and c) the importance of analyzing a loop pairing by establishing a suitable MO scenario. We propose to carry out three analyzes to show these important aspects:

Analysis 1): the methodology presented in this paper is applied to the linearized system and then directly on the non-linear system at operating point 1 ($\wp_1$) to compare the results in both cases. This is intended to show that the application of loop pairing techniques for linearized systems can be inaccurate when applied in a non-linear system.

Analysis 2): the methodology proposed in this paper is applied to the non-linear system at operating points 2 and 3 ($\wp_2$ and $\wp_3$) to compare these results with those obtained at operating point 1 ($\wp_1$). This analysis aims to show that the best loop pairing to control a non-linear system at an operating point must not necessarily coincide with the most suitable at another operating point.

Analysis 3): a multi-objective scenario with two design objectives (performance versus control effort) is analyzed and the subsequent MO scenario is expanded with four design objectives (performance versus control effort of each output and input independently). This shows the importance of establishing a suitable multi-objective scenario. In a suitable MO scenario, a designer does not have to aggregate output performances with control efforts. This avoids a possible loss of information when aggregating design objectives in a MOP, as well as the inconvenience of establishing aggregation weights.

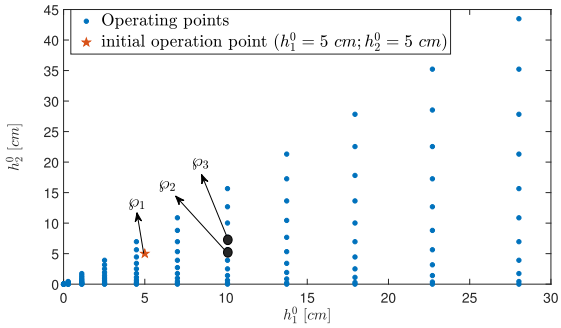

FIGURE 6. Proposed operating points for the coupled two-tank system.

In order to carry out these analyses, a set of feasible operating points for the system shown in Fig. 5 was generated. The operating points were obtained by increasing the pump voltage from 0 volts to 5 volts by 0.5 volts increments and the valve opening from 0 % to 1 % by 0.1 % increments, as shown in Fig. 6.

$\wp_1$ was selected as the initial operating point to begin the system analysis. At $\wp_1$ both tank levels have the same value ($h_1 = h_2 = 5\ cm$). Then $\wp_2$ was chosen to analyze the behavior of the system when h_1 varies and h_2 remains constant ($h_1 = 10\ cm; h_2 = 5\ cm$). Finally, $\wp_3$ was chosen to analyze the behavior of the system when both levels h_1 and h_2 shift from $\wp_1$ ($h_1 = 10\ cm; h_2 = 7.7\ cm$) (see Table 2). This intends to show the validity of the loop pairing of a non-linear system at different operating points.

The system was linearized at the operating points shown in Table 2. $G_1(s)$, $G_2(s)$ and $G_3(s)$ are shown in (21), (22) and (23), as shown at the bottom of this page, respectively. The relative gain array (RGA) was calculated to analyze the input-output pairing suggested by this technique to control each plant. RGA (Λ) clearly proposes a diagonal pairing for the decentralized control in each plant as shown in (24), as shown at the bottom of this page.

$$G_1(s) = \begin{bmatrix} \dfrac{0.02345s + 0.002098}{s^2 + 0.04276s + 0.0004431} & \dfrac{0.2512s}{s^2 + 0.04276s + 0.0004431} \\ \dfrac{0.08354}{s + 0.01764} & \dfrac{-0.2198}{s + 0.01764} \end{bmatrix} \tag{21}$$

$$G_2(s) = \begin{bmatrix} \dfrac{0.05142s + 0.002098}{s^2 + 0.0354s + 0.0003133} & \dfrac{0.3552s}{s^2 + 0.0354s + 0.0003133} \\ \dfrac{0.05907}{s + 0.01764} & \dfrac{-0.3108}{s + 0.01764} \end{bmatrix} \tag{22}$$

$$G_3(s) = \begin{bmatrix} \dfrac{0.03568s + 0.001694}{s^2 + 0.03192s + 0.0002518} & \dfrac{0.3568s}{s^2 + 0.03192s + 0.0002518} \\ \dfrac{0.07284}{s + 0.01424} & \dfrac{-0.3122}{s + 0.01424} \end{bmatrix} \tag{23}$$

$$\Lambda_{G_1} = \Lambda_{G_2} = \Lambda_{G_3} \begin{bmatrix} 1 & 0 \\ 0 & 1 \end{bmatrix} \tag{24}$$

TABLE 2. Operating points of the coupled two-tank system.

Operating points ($\wp$)	$\wp_1$	$\wp_2$	$\wp_3$
h_1^0	5 cm	10 cm	10 cm
h_2^0	5 cm	5 cm	7.7 cm
v^0	2.1181 V	2.9865 V	3 V
γ^0	0.1972	0.4323	0.3

To determine the optimal loop pairing, the technique proposed in this paper is applied to both the linearized system and the non-linear system. In both cases, two design concepts are proposed: $\mathbf{c}_1$ (diagonal concept) and $\mathbf{c}_2$ (off-diagonal concept) as shown in (25) and (26), and (29) and (30). To stabilize the system, 1-DOF PIs controllers with anti-windup are used as shown in (27) and (28), and (31) and (32).

$$\mathbf{c}_1 = \left[C^{c_1}_{h_1,\hat{u}_1}, C^{c_1}_{h_2,\hat{u}_2}\right] \tag{25}$$

$$\begin{bmatrix} v \\ \gamma \end{bmatrix} = \begin{bmatrix} 1 & 0 \\ 0 & 1 \end{bmatrix} \begin{bmatrix} \hat{u}_1 \\ \hat{u}_2 \end{bmatrix} \tag{26}$$

$$C^{c_1}_{h_1,\hat{u}_1} = \frac{K_1^{c1}(s + 1/Ti_1^{c1})}{s}, \quad C^{c_1}_{h_2,\hat{u}_2} = \frac{K_2^{c1}(s + 1/Ti_2^{c1})}{s} \tag{27}$$

$$\mathbf{x}^{c1} = \left[K_1^{c1}, Ti_1^{c1}, K_2^{c1}, Ti_2^{c1}\right] \tag{28}$$

$$\mathbf{c}_2 = \left[C^{c_2}_{h_1,\hat{u}_1}, C^{c_2}_{h_2,\hat{u}_2}\right] \tag{29}$$

$$\begin{bmatrix} v \\ \gamma \end{bmatrix} = \begin{bmatrix} 0 & 1 \\ 1 & 0 \end{bmatrix} \begin{bmatrix} \hat{u}_1 \\ \hat{u}_2 \end{bmatrix} \tag{30}$$

$$C^{c_2}_{h_1,\hat{u}_1} = \frac{K_1^{c2}(s + 1/Ti_1^{c2})}{s}, \quad C^{c_2}_{h_2,\hat{u}_2} = \frac{K_2^{c2}(s + 1/Ti_2^{c2})}{s} \tag{31}$$

$$\mathbf{x}^{c2} = \left[K_1^{c2}, Ti_1^{c2}, K_2^{c2}, Ti_2^{c2}\right] \tag{32}$$

Two MOPs are proposed with two design objectives each as shown in (33)–(39), where for $k = 1$ the MOP is associated with the design concept $\mathbf{c}_1$ or the diagonal concept, and for $k = 2$ it is associated with the design concept $\mathbf{c}_2$ or the off-diagonal concept.

Objective J_1 aggregates and evaluates the errors of the levels of each tank h_1 and h_2 by applying the IAE for reference input tracking (unit step response). Objective J_2 aggregates and evaluates the control efforts of the pump v and the valve γ by applying the IADU. Because the IADU of the pump was aggregated with the IADU of the valve, the pump control effort (v) was divided by its maximum voltage to assign to this variable a relative weight equivalent to the valve ($v = 0$ to 1). The bounds of the parameter vector of each controller $\mathbf{x}^{ck}$ are shown in Table 3.

$$\min_{\mathbf{x}^{ck}} \mathbf{J}(\mathbf{x}^{ck}) \tag{33}$$

$$\mathbf{J}(\mathbf{x}^{ck}) = \{J_1(\mathbf{x}^{ck}), J_2(\mathbf{x}^{ck})\} \tag{34}$$

$$J_1(\mathbf{x}^{ck}) = \int_0^{tf} |e_1| + |e_2| \Big|_{h_1=h_1^0+1cm}^{h_2=h_2^0} dt + \int_0^{tf} |e_1| + |e_2| \Big|_{h_1=h_1^0}^{h_2=h_2^0+1cm} dt \tag{35}$$

TABLE 3. Bounds of the decision vectors $\mathbf{x}^{c1}$ and $\mathbf{x}^{c2}$ for the first example-operating point 1.

Bounds of $\mathbf{x}^{ck}$-$\wp_1$				
$\mathbf{x}^{c1}$	K_1^{c1}	Ti_1^{c1}	K_2^{c1}	Ti_2^{c1}
$\underline{\mathbf{x}}^{c1}$	0.1	1	-10	5
$\overline{\mathbf{x}}^{c1}$	10	100	-0.1	100
$\mathbf{x}^{c2}$	K_1^{c2}	Ti_1^{c2}	K_2^{c2}	Ti_2^{c2}
$\underline{\mathbf{x}}^{c2}$	0.1	1	0.1	1
$\overline{\mathbf{x}}^{c2}$	20	100	30	50

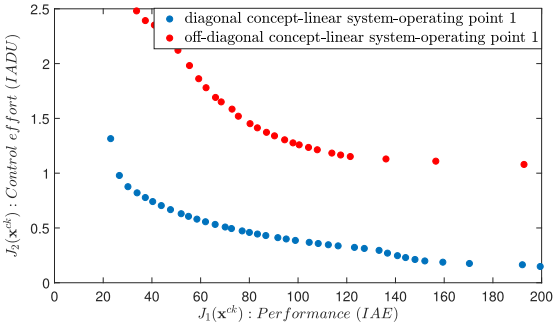

FIGURE 7. Pareto fronts for diagonal and off-diagonal design concepts for the linear system.

$$J_2(\mathbf{x}^{ck}) = \int_0^{tf} \left|\frac{du_1}{dt}\right| + \left|\frac{du_2}{dt}\right| \Big|_{h_1=h_1^0+1cm}^{h_2=h_2^0} dt + \int_0^{tf} \left|\frac{du_1}{dt}\right| + \left|\frac{du_2}{dt}\right| \Big|_{h_1=h_1^0}^{h_2=h_2^0+1cm} dt \tag{36}$$

$$t_f = 400\ seconds$$

$$\underline{\mathbf{x}}^{ck} \leq \mathbf{x}^{ck} \leq \overline{\mathbf{x}}^{ck} \tag{37}$$

$$J_1(\mathbf{x}^{ck}) < 200; J_2(\mathbf{x}^{ck}) < 14 \tag{38}$$

$$\mathbf{x}^{ck} = \left[K_1^{ck}, Ti_1^{ck}, K_2^{ck}, Ti_2^{ck}\right] \tag{39}$$

A. ANALYSIS 1: LINEARIZED SYSTEM VERSUS NON-LINEAR SYSTEM

In this first analysis, the loop pairing technique proposed in this paper is first applied to the linearized system and then to the non-linear system.

By optimizing the MOPs proposed in (33)–(39) for the linearized system at the operating point 1, the Pareto fronts shown in Fig. 7 are obtained. It is possible to observe that the diagonal design concept dominates the off-diagonal concept. Therefore, in this case it is suggested selecting a diagonal input-output pairing for the decentralized control of the MIMO system (this result is in accordance with the proposed RGA).

The same procedure was applied directly to the non-linear system. Pareto fronts for each design concept are shown in Fig. 8. It is possible to observe that the scenario has changed radically, and the off-diagonal design concept now dominates the diagonal concept.

From this simple analysis it is concluded that when applying a loop pairing technique on a linearized system, the results obtained may not be coincident with those that would be

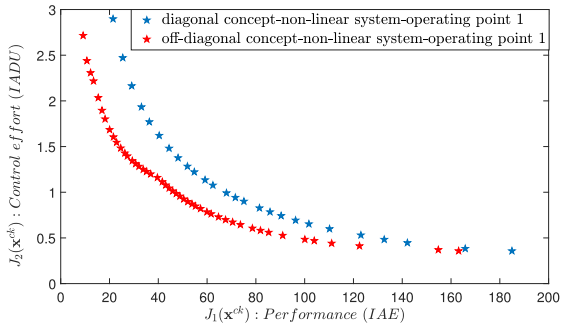

FIGURE 8. Pareto fronts for diagonal and off-diagonal design concepts for the non-linear system.

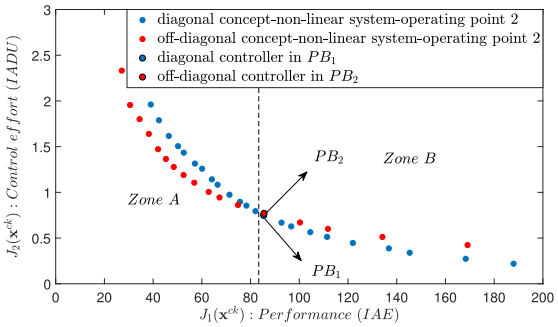

FIGURE 9. Pareto fronts for diagonal and off-diagonal design concepts for the non-linear system for operating point 2.

TABLE 4. Bounds of the decision vectors $\mathbf{x}^{c1}$ and $\mathbf{x}^{c2}$ for the first example, operating points 2 and 3.

Bounds of $\mathbf{x}^{ck}$-$\wp_2$ and $\wp_3$				
$\mathbf{x}^{c1}$	K_1^{c1}	Ti_1^{c1}	K_2^{c1}	Ti_2^{c1}
$\underline{\mathbf{x}}^{c1}$	0.1	1	-50	1
$\overline{\mathbf{x}}^{c1}$	50	200	-0.1	200
$\mathbf{x}^{c2}$	K_1^{c2}	Ti_1^{c2}	K_2^{c2}	Ti_2^{c2}
$\underline{\mathbf{x}}^{c2}$	0.01	1	0.01	1
$\overline{\mathbf{x}}^{c2}$	50	200	100	200

obtained by applying the same technique directly on the non-linear system. This gives a significant advantage to the techniques that can be applied directly to non-linear systems versus those techniques that need to linearize the plant to be applied.

B. ANALYSIS 2: NON-LINEAR SYSTEM AT DIFFERENT OPERATING POINT

In this second analysis, the input-output pairings to control the MIMO system shown in Fig. 5 are analyzed. The behavior of the system when the tanks decrease their levels is analyzed (h_1 and h_2 decrease 1 *cm* from their operating points).

The diagonal and off-diagonal design concepts, the 1-DOF PIs controllers, and the MOPs proposed in this scenario are the same as in operating point 1 (Analysis 1). The bounds of the parameter vector $\mathbf{x}^{ck}$ were expanded and are shown in Table 4.

The Pareto fronts of each design concept applying the methodology proposed directly on the non-linear system for operating point 2 are shown in Fig. 9. Unlike operating point 1 (see Fig. 7 and Fig. 8), no design concept completely dominates the other at operating point 2.

It is possible to analyze in greater detail the compromises between these Pareto fronts by establishing two zones in the objectives space (zone A and zone B) where each zone has different characteristics as shown in Fig. 9.

Zone A corresponds to the region where the off-diagonal concept dominates the diagonal concept. In this zone are the controllers with the best performance for reference tracking of the levels h_1 and h_2, and with greater control efforts on pump v and valve γ.

Zone B corresponds to the region where the diagonal concept dominates the off-diagonal concept. In this zone are

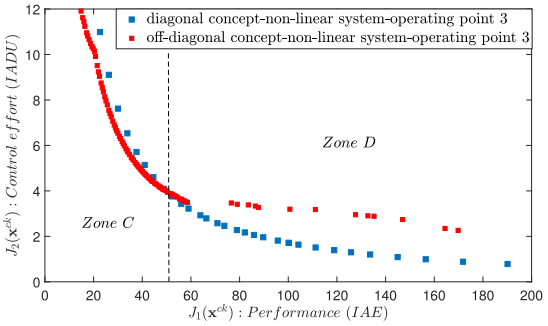

FIGURE 10. Pareto fronts for diagonal and off-diagonal design concepts for the non-linear system for operating point 3.

the controllers with the lowest performance for reference tracking in h_1 and h_2 but with less aggressive control efforts for v and γ. Therefore, at operating point 2 the best loop pairing to control the system will depend on the designer's preferences a posteriori.

The Pareto fronts (one for each design concept) obtained when the proposed methodology is applied to the non-linear system at operating point 3 are shown in Fig.10. The scenario is equivalent to the one obtained at operating point 2, where no design concept completely dominates the other. (In zone C, off-diagonal loop pairing is preferable and, in zone D, diagonal loop pairing is preferable).

This disagreement of results between operating points allows us to conclude that in a non-linear system the best loop pairing will depend on the operating point at which the system is analyzed.

C. ANALYSIS 3: SUITABLE MULTI-OBJECTIVE SCENARIO

Two scenarios are compared in this third analysis: the scenario with two objectives at operating point 2 presented in analysis 2; and another with four design objectives at the same operating point. The advantages and disadvantages of both scenarios are analyzed.

In analysis 2, MOPs with two design objectives are proposed (J_1: IAE of h_1 and h_2; J_2: IADU of v and γ) to find an optimal loop pairing. A fundamental advantage of this scenario is that it is easy to compare Pareto fronts in each multi-objective problem in the bi-dimensional space as shown in Fig. 9. However, a scenario of only two design objectives

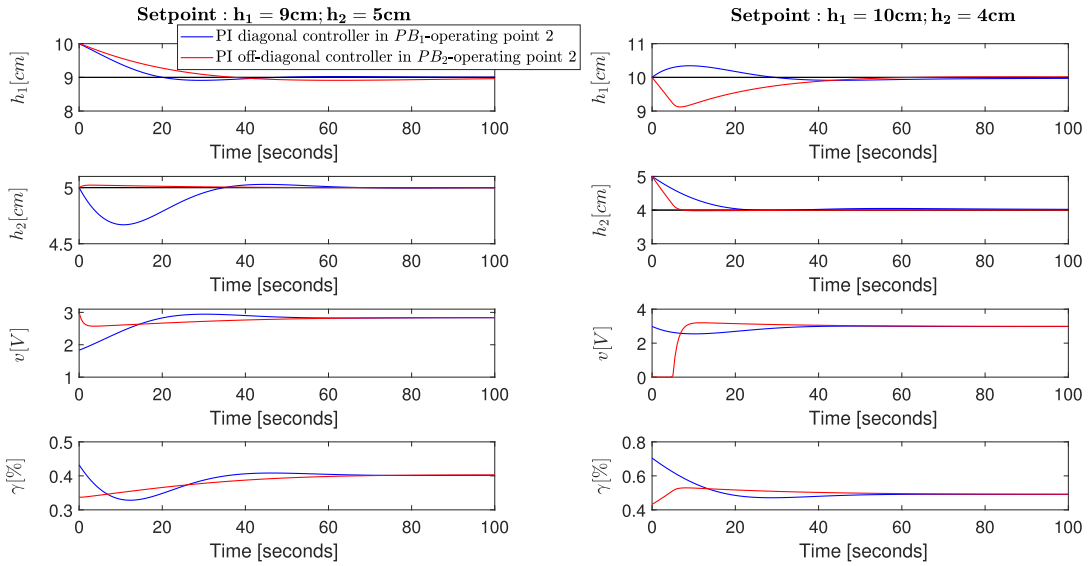

FIGURE 11. PIs controllers responses in PB_1 and PB_2 in non-linear system for the operating point 2.

TABLE 5. PIs diagonal and off-diagonal controllers selected in Fig. 9.

PI off-diagonal controller		PI diagonal controller	
Parameters	PB_2	Parameters	PB_1
K_1^{c2}	0.0953	K_1^{c1}	1.1549
Ti_1^{c2}	28.17	Ti_1^{c1}	63.78
K_2^{c2}	17.68	K_2^{c1}	-0.2724
Ti_2^{c2}	57.50	Ti_2^{c1}	52.95
$J_1(\mathbf{x}^{c2})$	85.50	$J_1(\mathbf{x}^{c1})$	85.38
$J_2(\mathbf{x}^{c2})$	0.7705	$J_2(\mathbf{x}^{c1})$	0.7481

has the disadvantage that there is information that can be masked by aggregating errors from different outputs into a single design objective J_1. Also, by aggregating the IADU of v and γ into a single design objective J_2, two system variables that physically represent quantities with different units of measurement are mixed. This could hide information about their behaviors and hinder a correct interpretation.

To analyze the differences between both loop pairings, a controller from each design concept is chosen: PB_1 of the diagonal concept and PB_2 of the off-diagonal concept as shown in Fig. 9. Table 5 shows the performance of the controllers in PB_1 and PB_2. It is observed that both controllers have very similar performances, since $J_1(\mathbf{x}^{c2}) \approx J_1(\mathbf{x}^{c1})$ and $J_2(\mathbf{x}^{c2}) \approx J_2(\mathbf{x}^{c1})$. A designer when analyzing these objectives may not be able to detect that the controllers are different. The responses of these controllers are shown in Fig. 11. The diagonal controller has better performance for reference tracking in h_1 and the off-diagonal controller for reference tracking in h_2. This is not detectable in design objective J_1 because this objective mixes the performance of h_1 and h_2.

To analyze in greater detail the performances of each system output, the methodology enables the generation of a new scenario with four design objectives. In this scenario, the output and input variables are not mixed, and the trade-off that exists between the IAE of output h_1 and the IAE of h_2 are analyzed independently, as well as the IADU of each input v and γ.

By analyzing the trade-off between the IADU of the pump with the IADU of the valve independently, a better interpretation of the MOPs and a greater physical sense of the system is achieved. In this scenario, it is not necessary to resize the control effort v because it does not mix with the control effort γ. Two MOPs with four design objectives each are proposed according to (40)–(48). The bounds of the decision vector $\mathbf{x}^{ck}$ are the same as in Table 3.

$$\min_{\mathbf{x}^{ck}} \mathbf{J}(\mathbf{x}^{ck}) \tag{40}$$

$$J(\mathbf{x}^{ck}) = \{J_1(\mathbf{x}^{ck}), J_2(\mathbf{x}^{ck}), J_3(\mathbf{x}^{ck}), J_4(\mathbf{x}^{ck})\} \tag{41}$$

$$J_1(\mathbf{x}^{ck}) = \int_0^{t_f} |e_1|\Big|_{h_1=h_1^0-1cm}^{h_2=h_2^0} dt + \int_0^{t_f} |e_1|\Big|_{h_1=h_1^0}^{h_2=h_2^0-1cm} dt \tag{42}$$

$$J_2(\mathbf{x}^{ck}) = \int_0^{t_f} |e_2|\Big|_{h_1=h_1^0-1cm}^{h_2=h_2^0} dt + \int_0^{t_f} |e_2|\Big|_{h_1=h_1^0}^{h_2=h_2^0-1cm} dt \tag{43}$$

$$J_3(\mathbf{x}^{ck}) = \int_0^{t_f} \left|\frac{du_1}{dt}\right|\Big|_{h_1=h_1^0-1cm}^{h_2=h_2^0} dt + \int_0^{t_f} \left|\frac{du_1}{dt}\right|\Big|_{h_1=h_1^0}^{h_2=h_2^0-1cm} dt \tag{44}$$

$$J_4(\mathbf{x}^{ck}) = \int_0^{t_f} \left|\frac{du_2}{dt}\right|\Big|_{h_1=h_1^0-1cm}^{h_2=h_2^0} dt + \int_0^{t_f} \left|\frac{du_2}{dt}\right|\Big|_{h_1=h_1^0}^{h_2=h_2^0-1cm} dt \tag{45}$$

$$t_f = 400\ seconds$$

$$\underline{\mathbf{x}}^{ck} \leq \mathbf{x}^{ck} \leq \overline{\mathbf{x}}^{ck} \tag{46}$$

$$J_1(\mathbf{x}^{ck}) < 200; \quad J_2(\mathbf{x}^{ck}) < 200;$$

$$J_3(\mathbf{x}^{ck}) < 14; \quad J_4(\mathbf{x}^{ck}) < 14 \tag{47}$$

$$\mathbf{x}^{ck} = \left[K_1^{ck}, Ti_1^{ck}, K_2^{ck}, Ti_2^{ck}\right] \tag{48}$$

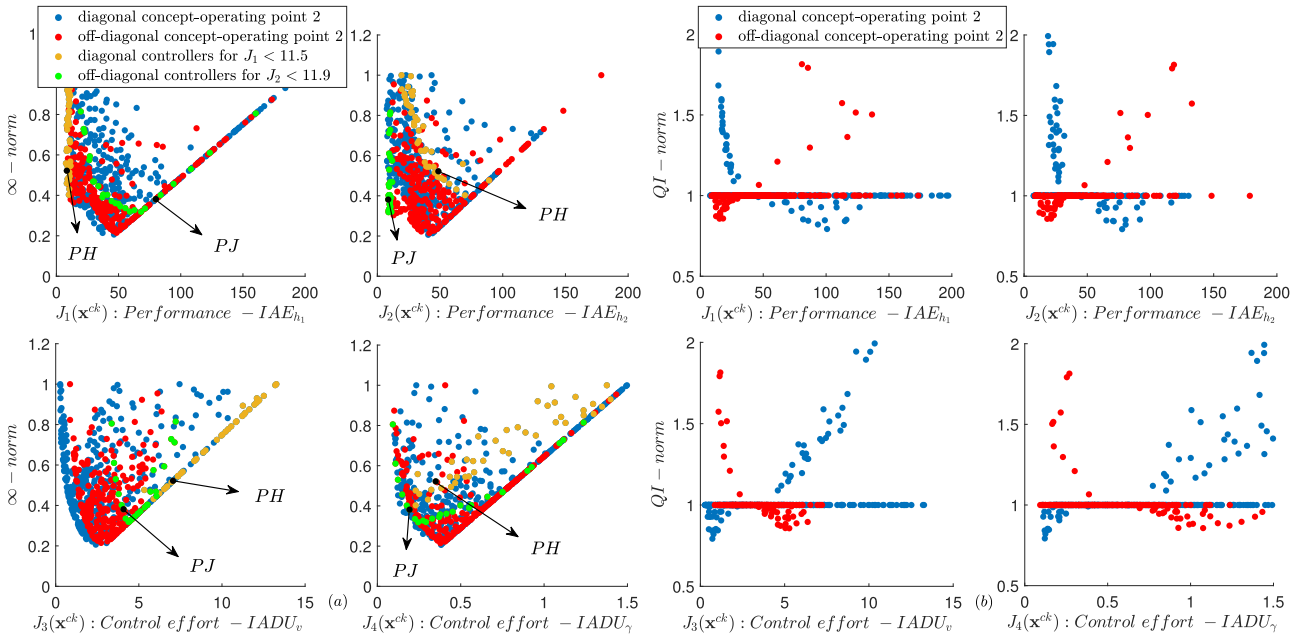

FIGURE 12. Pareto fronts and comparison of design concepts using *level diagram* for operating point 2. The solutions *PH* and *PJ* were selected to analyze their trade-off. (a) design concepts using ∞-norm. (b) design concepts using *QI*-norm. Only the solutions where $QI < 2$ has been plotted.

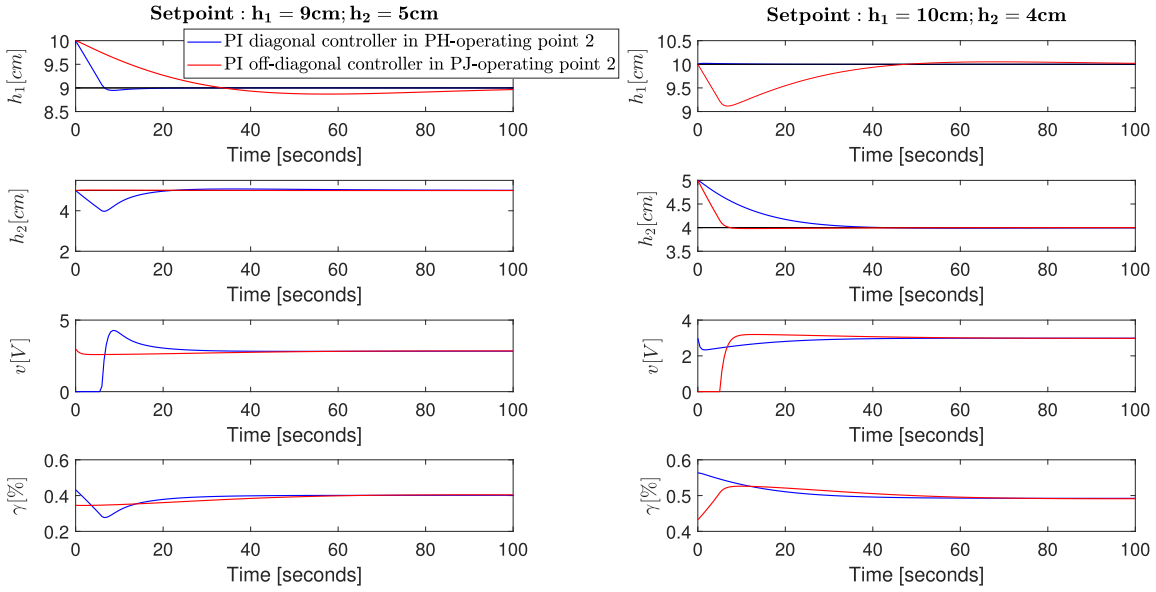

FIGURE 13. PIs controllers responses in *PH* and *PJ* for the operating point 2.

The Pareto fronts associated with the diagonal ($k = 1$) and off-diagonal ($k = 2$) design concepts obtained with the optimization of each MOP proposed in (40) are shown in Fig. 12 (a). It is possible to observe that the diagonal concept achieves better performance for h_1 than the off-diagonal concept (brown solutions). The off-diagonal concept achieves a better performance than the diagonal concept for h_2 (green solutions). In Fig. 12 (b) when applying the QI-norm, it is observed that there is a zone where the diagonal concept dominates the off-diagonal concept ($QI_{diagonal} < 1$) and a different zone where the opposite is true ($QI_{off-diagonal} < 1$).

One controller from each design concept was selected among those that have the best performances for each output (*PH* and *PJ*) and their responses are shown in Fig. 13. The diagonal controller is better for reference tracking in h_1, the opposite is true for the off-diagonal controller as shown in Fig. 13. This can be quantified in objectives $J_1(\mathbf{x}^{ck})$ and $J_2(\mathbf{x}^{ck})$ as shown in Table 6. The off-diagonal controller has softer control efforts than the diagonal controller as shown in objectives $J_3(\mathbf{x}^{ck})$ and $J_4(\mathbf{x}^{ck})$ in Table 6.

This scenario has as its main advantage that it offers detailed information on the trade-off between IAE and IADU of each output and each input respectively. A designer can

TABLE 6. PI diagonal and off-diagonal controllers selected in Figure 12.

PI off-diagonal controller		PI diagonal controller	
$Parameters$	PJ	$Parameters$	PH
K_1^{c2}	0.087	K_1^{c1}	32.50
Ti_1^{c2}	21.70	Ti_1^{c1}	30.63
K_2^{c2}	18.19	K_2^{c1}	-0.131
Ti_2^{c2}	54.65	Ti_2^{c1}	23.61
$J_1(\mathbf{x}^{c2})$	80.01	$J_1(\mathbf{x}^{c1})$	**8.43**
$J_2(\mathbf{x}^{c2})$	**8.69**	$J_2(\mathbf{x}^{c1})$	48.63
$J_3(\mathbf{x}^{c2})$	4.08	$J_3(\mathbf{x}^{c1})$	7.06
$J_4(\mathbf{x}^{c2})$	0.193	$J_4(\mathbf{x}^{c1})$	0.35

choose in this scenario an input-output pairing with independent preferences over these indices to control the coupled two-tank system. As a disadvantage, the analysis in the decision making stage is more complex compared to a scenario of only two design objectives. Another advantage is that having more information on each MOP helps a designer choose an optimal solution with greater certainty (with satisfactory performances according to certain preferences).

It can be seen in this first example that the optimal input-output pairing for the decentralized control of the non-linear multivariable system shown in Fig. 5 depends on the following aspects: the operating point in which the system is analyzed and its dynamics at that point; the design objectives proposed for each design concept; the designer's preferences relative to the design objectives; and the type of controller structure. A relevant aspect in this example is that by applying the methodology proposed in this paper in the linearized system, and subsequently applying the methodology directly to the non-linear system, Pareto fronts with differing dominances are obtained. Therefore, it is considered important to extend the methodology proposed in [46] for its application in non-linear multivariable systems.

V. EXAMPLE 2: NON-LINEAR QUADRUPLE-TANK SYSTEM (2 × 2)

In this example, the non-linear quadruple-tank system used in [49] is analyzed. The schematic diagram of the system is shown in Fig. 14 and the first principle non-linear model is shown in (49)-(52).

$$\frac{dh_1}{dt} = -\frac{a_1}{A_1}\sqrt{2gh_1} + \frac{a_3}{A_1}\sqrt{2gh_3} + \frac{\gamma_1 k_1}{A_1}v_1 \tag{49}$$

$$\frac{dh_2}{dt} = -\frac{a_2}{A_2}\sqrt{2gh_2} + \frac{a_4}{A_2}\sqrt{2gh_4} + \frac{\gamma_2 k_2}{A_2}v_2 \tag{50}$$

$$\frac{dh_3}{dt} = -\frac{a_3}{A_3}\sqrt{2gh_3} + \frac{(1-\gamma_2)k_2}{A_3}v_2 \tag{51}$$

$$\frac{dh_4}{dt} = -\frac{a_4}{A_4}\sqrt{2gh_4} + \frac{(1-\gamma_1)k_1}{A_4}v_1 \tag{52}$$

where:

A_i: cross-section of tank i, i=1 to 4.
a_i, cross-section of the outlet holes i.
h_i: water levels.
γ_i: Valve i opening/closing coefficients, i=1 to 2.
v_i: voltages applied to the pumps i.
$k_i v_i$: flows of pumps i.
g: acceleration of gravity.

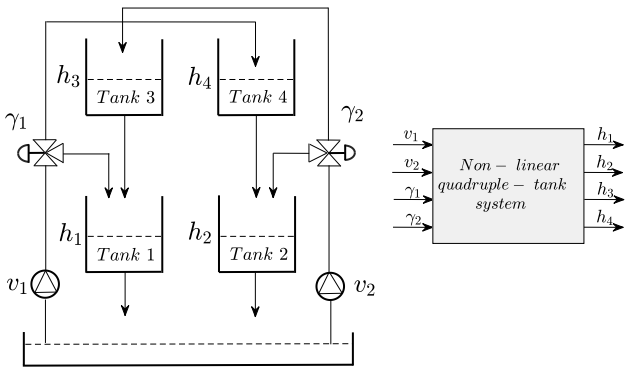

FIGURE 14. Schematic diagram of quadruple-tank system.

TABLE 7. Parameters for the quadruple-tank system.

Parameter	Value
A_1, A_3	28 cm^2
A_2, A_4	32 cm^2
a_1, a_3	0.071 cm^2
a_2, a_4	0.057 cm^2
k_1	3.14 cm^3/Vs
k_2	3.29 cm^3/Vs
γ_1	0.43
γ_2	0.34
g	981 cm/s^2

The system actuators have the constrains shown in (53).

$$0 \leq v \leq 7.2\,V,\ 0 \leq \gamma \leq 1 \tag{53}$$

Model parameters are shown in Table 7.

For this example, outputs h_1 and h_2 are controlled through pumps v_1 and v_2, the valves coefficients are $\gamma_1 = 0.43$ and $\gamma_2 = 0.34$. With these system conditions, the scenario proposed in [49] is obtained, which is compared with other scenarios generated with the methodology proposed in this paper. The system under these valve conditions has a non-minimal phase behavior and this adds complexity to the decentralized control [49].

The operating point proposed in [49] was used here to linearize the system and contrast the methodology proposed in this paper over a model of a real laboratory process (the scenario proposed in [49] was generated and compared with other scenarios). The operating point is shown in Table 8.

RGA (Λ) proposes for this operating point an off-diagonal pairing for the decentralized control of the linearized plant as shown in (54), as shown at the bottom of the next page. An extension of RGA to non linear systems [13] suggests a diagonal pairing for the decentralized control of the quadruple-tank system. The extended RGA is shown in (55), as shown at the bottom of the next page. The non-linear RGA (NRGA, [14], [15]) for the system is shown in (56), as shown at the bottom of the next page. NRGA suggests considering the operating point and parameters of the quadruple-tank system when choosing a loop pairing. When applying NRGA at the operating point shown in Table 8, an off-diagonal pairing to control the quadruple-tank system is suggested. It is also

TABLE 8. Operating point of the qudruple-tank system.

Operating point $\wp$	
h_1^0	12.44 cm
h_2^0	13.17 cm
h_3^0	4.73 cm
h_4^0	4.99 cm
v_1^0	3.15 V
v_2^0	3.15 V

suggested in [15] to analyze the closed-loop response to study the performance of each possible loop pairing (simulating the diagonal and off-diagonal controllers).

The methodology proposed in this paper was applied directly to the non-linear system in order to analyze in detail how to choose the most appropriate input-output pairing. Two design concepts $\mathbf{c}_1$ (diagonal concept) and $\mathbf{c}_2$ (off-diagonal concept) are proposed, 1-DOF PIs controllers with anti-windup equivalent to those proposed in [49] are used as shown in (57)–(64), as shown at the bottom of this page.

For each design concept a MOP is proposed. Each MOP has four design objectives as shown in (65)–(73). Two objectives independently analyze the IAE of outputs h_1 and h_2 and the other objectives analyze the IADU of each input v_1 and v_2. Because the system has non-minimal phase behavior, it is slower to stabilize and the simulation time t_f is extended.

$$\min_{\mathbf{x}^{ck}} \mathbf{J}(\mathbf{x}^{ck}) \tag{65}$$

$$\mathbf{J}(\mathbf{x}^{ck}) = \{J_1(\mathbf{x}^{ck}), J_2(\mathbf{x}^{ck}), J_3(\mathbf{x}^{ck}), J_4(\mathbf{x}^{ck})\} \tag{66}$$

$$J_1(\mathbf{x}^{ck}) = \int_0^{t_f} |e_1| \Big|_{h_1=h_1^0+1cm}^{h_2=h_2^0} dt + \int_0^{t_f} |e_1| \Big|_{h_1=h_1^0}^{h_2=h_2^0+1cm} dt \tag{67}$$

$$J_2(\mathbf{x}^{ck}) = \int_0^{t_f} |e_2| \Big|_{h_1=h_1^0+1cm}^{h_2=h_2^0} dt + \int_0^{t_f} |e_2| \Big|_{h_1=h_1^0}^{h_2=h_2^0+1cm} dt \tag{68}$$

$$J_3(\mathbf{x}^{ck}) = \int_0^{t_f} \left|\frac{du_1}{dt}\right| \Big|_{h_1=h_1^0+1cm}^{h_2=h_2^0} dt + \int_0^{t_f} \left|\frac{du_1}{dt}\right| \Big|_{h_1=h_1^0}^{h_2=h_2^0+1cm} dt \tag{69}$$

$$J_4(\mathbf{x}^{ck}) = \int_0^{t_f} \left|\frac{du_2}{dt}\right| \Big|_{h_1=h_1^0+1cm}^{h_2=h_2^0} dt + \int_0^{t_f} \left|\frac{du_2}{dt}\right| \Big|_{h_1=h_1^0}^{h_2=h_2^0+1cm} dt \tag{70}$$

$$\Lambda = \begin{bmatrix} -0.6357 & 1.6357 \\ 1.6357 & -0.6357 \end{bmatrix} \tag{54}$$

$$\Lambda_{NL} = \begin{bmatrix} \frac{\gamma_1 k_1}{A_1} & 0 \\ 0 & \frac{\gamma_2 k_2}{A_2} \end{bmatrix} .* \begin{bmatrix} \frac{\gamma_1 k_1}{A_1} & 0 \\ 0 & \frac{\gamma_2 k_2}{A_2} \end{bmatrix}^{-T} = \begin{bmatrix} 1 & 0 \\ 0 & 1 \end{bmatrix} \tag{55}$$

$$\Lambda_{NRGA} = \begin{bmatrix} \frac{1}{1 - \frac{(1-\gamma_1)(1-\gamma_2)}{\gamma_1\gamma_2}\sqrt{\frac{h_1 h_2}{h_3 h_4}}} & \frac{1}{1 - \frac{\gamma_1\gamma_2}{(1-\gamma_1)(1-\gamma_2)}\sqrt{\frac{h_3 h_4}{h_1 h_2}}} \\ \frac{1}{1 - \frac{\gamma_1\gamma_2}{(1-\gamma_1)(1-\gamma_2)}\sqrt{\frac{h_3 h_4}{h_1 h_2}}} & \frac{1}{1 - \frac{(1-\gamma_1)(1-\gamma_2)}{\gamma_1\gamma_2}\sqrt{\frac{h_1 h_2}{h_3 h_4}}} \end{bmatrix} = \begin{bmatrix} -0.1730 & 1.1730 \\ 1.1730 & -0.1730 \end{bmatrix} \tag{56}$$

$$\mathbf{c}_1 = \begin{bmatrix} C^{c1}_{h_1,\hat{u}_1}, & C^{c1}_{h_2,\hat{u}_2} \end{bmatrix} \tag{57}$$

$$\begin{bmatrix} v_1 \\ v_2 \end{bmatrix} = \begin{bmatrix} 1 & 0 \\ 0 & 1 \end{bmatrix} \begin{bmatrix} \hat{u}_1 \\ \hat{u}_2 \end{bmatrix} \tag{58}$$

$$C^{c1}_{h_1,\hat{u}_1} = \frac{K_1^{c1}(s + 1/Ti_1^{c1})}{s}, \quad C^{c1}_{h_2,\hat{u}_2} = \frac{K_2^{c1}(s + 1/Ti_2^{c1})}{s} \tag{59}$$

$$\mathbf{x}^{c1} = \begin{bmatrix} K_1^{c1}, Ti_1^{c1}, K_2^{c1}, Ti_2^{c1} \end{bmatrix} \tag{60}$$

$$\mathbf{c}_2 = \begin{bmatrix} C^{c_2}_{h_1,\hat{u}_1}, & C^{c_2}_{h_2,\hat{u}_2} \end{bmatrix} \tag{61}$$

$$\begin{bmatrix} v_1 \\ v_2 \end{bmatrix} = \begin{bmatrix} 0 & 1 \\ 1 & 0 \end{bmatrix} \begin{bmatrix} \hat{u}_1 \\ \hat{u}_2 \end{bmatrix} \tag{62}$$

$$C^{c_2}_{h_1,\hat{u}_1} = \frac{K_1^{c2}(s + 1/Ti_1^{c2})}{s}, \quad C^{c_2}_{h_2,\hat{u}_2} = \frac{K_2^{c2}(s + 1/Ti_2^{c2})}{s} \tag{63}$$

$$\mathbf{x}^{c2} = \begin{bmatrix} K_1^{c2}, Ti_1^{c2}, K_2^{c2}, Ti_2^{c2} \end{bmatrix} \tag{64}$$

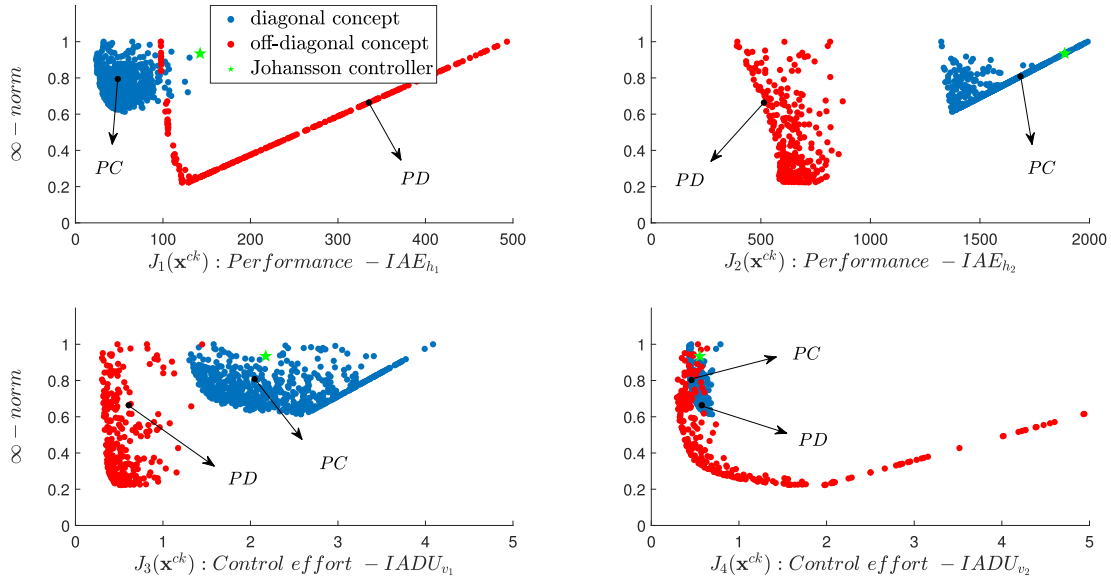

FIGURE 15. Pareto fronts using level diagram for second example. The solutions *PC*, *PD* were selected to analyze their trade-off.

TABLE 9. Bounds of the decision vectors $\mathbf{x}^{c1}$ and $\mathbf{x}^{c2}$ for the second example.

Bounds of $\mathbf{x}^{ck}$				
$\mathbf{x}^{c1}$	K_1^{c1}	Ti_1^{c1}	K_2^{c1}	Ti_2^{c1}
$\underline{\mathbf{x}}^{c1}$	0.1	10	-1	5
$\overline{\mathbf{x}}^{c1}$	3	50	-0.01	200
$\mathbf{x}^{c2}$	K_1^{c2}	Ti_1^{c2}	K_2^{c2}	Ti_2^{c2}
$\underline{\mathbf{x}}^{c2}$	0.1	10	0.1	50
$\overline{\mathbf{x}}^{c2}$	5	100	1	200

$$t_f = 1500\ seconds$$

$$\underline{\mathbf{x}}^{ck} \leq \mathbf{x}^{ck} \leq \overline{\mathbf{x}}^{ck} \tag{71}$$

$$J_1(\mathbf{x}^{ck}) < 500; \quad J_2(\mathbf{x}^{ck}) < 2000;$$

$$J_3(\mathbf{x}^{ck}) < 5; \quad J_4(\mathbf{x}^{ck}) < 5 \tag{72}$$

$$\mathbf{x}^{ck} = \left[K_1^{ck}, Ti_1^{ck}, K_2^{ck}, Ti_2^{ck}\right] \tag{73}$$

The bounds of the vector $\mathbf{x}^{ck}$ are shown in Table 9.

After the optimization process of each MOP, the Pareto fronts were obtained as shown in Fig. 15. The diagonal concept has a better performance for reference tracking of the output h_1 compared to the off-diagonal concept because the zone where $J_1(\mathbf{x}^{c1}) < 96.43$ is only covered by this design concept.

The off-diagonal concept has a better performance for reference tracking at the output h_2 compared to the diagonal concept because it covers a region where $J_2(\mathbf{x}^{c2}) < 873.8$ that the diagonal concept does not cover.

The control efforts of the pump v_1 of the diagonal concept ($J_3(\mathbf{x}^{c1}) > 1.302$) are greater than those of the off-diagonal concept ($J_3(\mathbf{x}^{c2}) < 1.448$). The control efforts of the pump v_2 share the same zone in the Pareto front of both design concepts ($0.2916 \leq J_4(\mathbf{x}^{ck}) \leq 0.789$). The control efforts of the off-diagonal concept where $J_4(\mathbf{x}^{c2}) > 0.789$ correspond to the best performances of h_1.

A solution of each design concept (*PC* and *PD*) was chosen to analyze its performance and compare them with the solution proposed in [49]. A step reference input was applied starting from the system operating point, the responses are shown in Fig. 16 and their performances in Table 10.

The off-diagonal controller in *PD* has a better performance for the output h_2 compared to the diagonal controller in *PC* as shown in Table 10 ($J_2(\mathbf{x}^{c2}) \ll J_2(\mathbf{x}^{c1})$) and in Fig. 16. The opposite is true, that is the diagonal controller in *PC* has a better performance in the output h_1, ($J_1(\mathbf{x}^{c1}) \ll J_1(\mathbf{x}^{c2})$) (see Table 10 and Fig.16). The control effort of the pump v_1 is smoother for the diagonal controller in *PD* compared to the off-diagonal controller in *PC* ($J_3(\mathbf{x}^{c2}) < J_3(\mathbf{x}^{c1})$), the opposite is true with the control effort of the pump v_2 for the controller in *PC* ($J_4(\mathbf{x}^{c1}) < J_4(\mathbf{x}^{c2})$).

The diagonal controller in *PC* tuned with the multi-objective technique proposed in this paper achieves better performance in all design objectives than the diagonal controller proposed in [49] as shown in Table 10 and in Fig. 16.

There is a conflict in this example between the two loop pairings available to control the quadruple-tank system proposed in [49]. An input-output pairing is better to control the level of one of the tanks and vice versa. It is interesting to note that with the proposed methodology it is possible to find a diagonal controller with better performance than the diagonal controller proposed in [49]. This is evidenced in the Pareto fronts and design objectives shown in Fig. 15 and in Table 10 respectively, as well as in the system responses shown in Fig. 16.

VI. EXAMPLE 3: NON-LINEAR QUADRUPLE-TANK SYSTEM (4 × 4)

In this example, the system proposed in [49] is analyzed and shown in Fig. 14. But now the four levels of the tanks

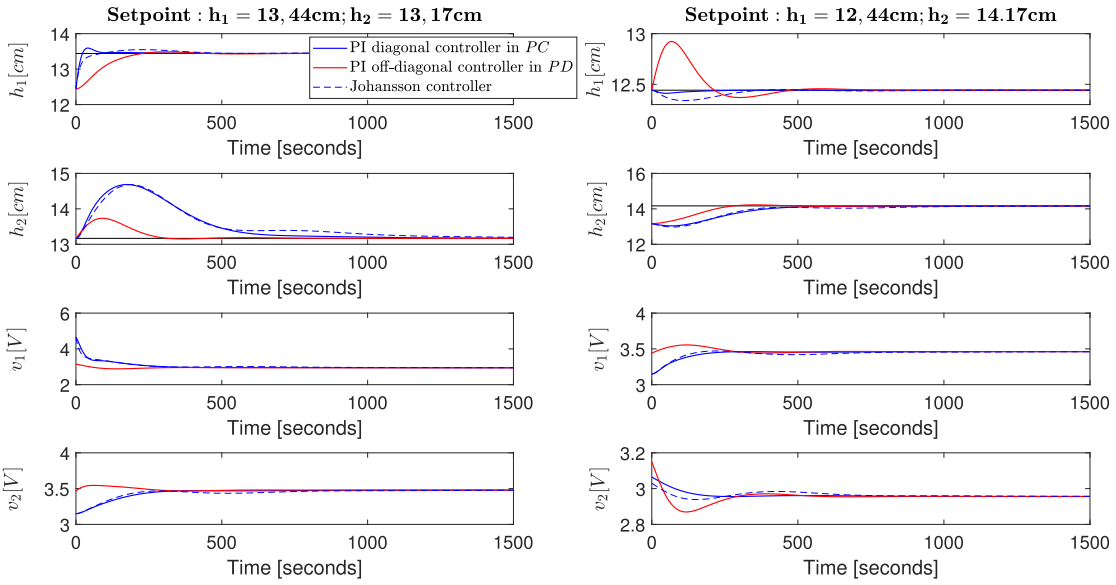

FIGURE 16. Responses of the controllers in *PC*, *PD* and the proposed controller in [49]. The outputs of the controller proposed by [49] are converted from volts to centimeters.

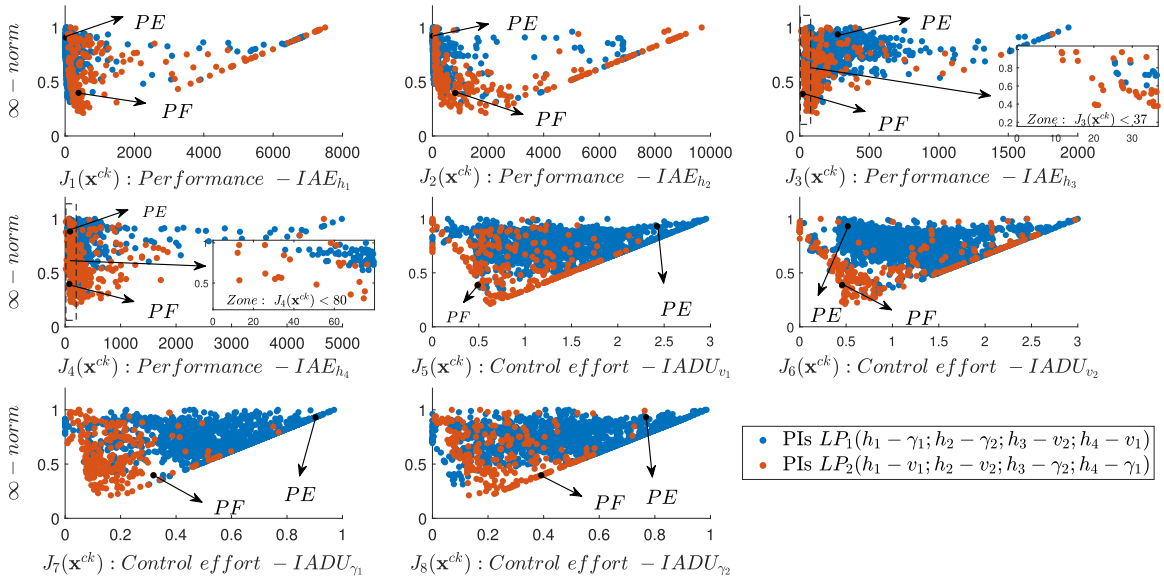

FIGURE 17. Representation of Pareto fronts for loop pairings LP_1 and LP_2 using LD.

(h_1, h_2, h_3, h_4) are controlled through the available pumps and valves $(v_1, v_2, \gamma_1, \gamma_2)$. The RGA (Λ) of the linearized system at the operating point proposed in [49] (see Table 8) is shown in (74).

$$\Lambda = \begin{array}{c} \\ h_1 \\ h_2 \\ h_3 \\ h_4 \end{array} \begin{array}{c} \begin{array}{cccc} v_1 & v_2 & \gamma_1 & \gamma_2 \end{array} \\ \begin{pmatrix} 0.43 & 0 & \mathbf{0.57} & 0 \\ 0 & 0.34 & 0 & \mathbf{0.66} \\ 0 & \mathbf{0.66} & 0 & 0.34 \\ \mathbf{0.57} & 0 & 0.43 & 0 \end{pmatrix} \end{array} \tag{74}$$

RGA suggests the loop pairing that is highlighted in bold as shown in (74) to control h_1 with valve γ_1, h_2 with valve γ_2, h_3 with pump v_2, and h_4 with pump v_1. However, there is another feasible input-output pairing to control h_1 with v_1, h_2 with v_2, h_3 with γ_2, and h_4 with γ_1. The performance of each loop pairing is analyzed with the technique proposed in this paper to better choose an optimal input-output pairing to control this MIMO system. Two design concepts: $\mathbf{c}_1$ (loop pairing LP_1); and $\mathbf{c}_2$ (loop pairing LP_2), are proposed using 1-DOF PIs controllers with anti-windup as shown in (75)–(82). A MOP for each design concept is proposed. Each MOP has eight design objectives as shown in (83)-(89). Four objectives analyze the trade-off between the IAE of each output (h_1, h_2, h_3, h_4) and the remaining four

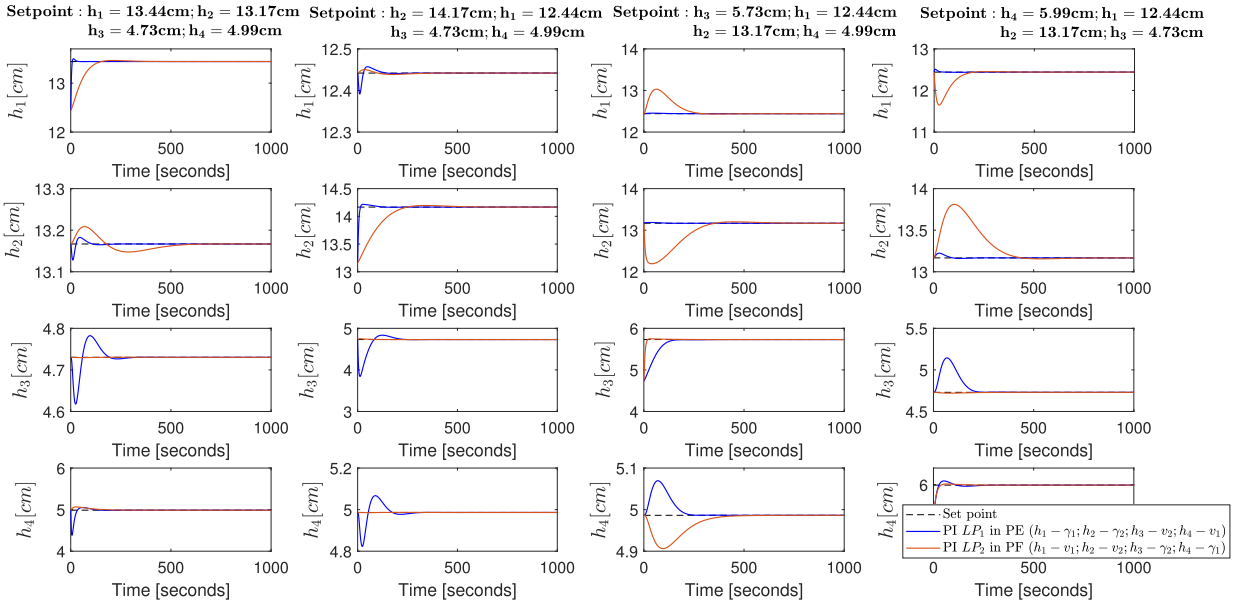

FIGURE 18. System outputs for the controllers in *PE* and *PF*.

objectives analyze the trade-off between the IADU of each input $(v_1, v_2, \gamma_1, \gamma_2)$. When proposing MOPs with eight design objectives, the performance of each input-output pairing to control the system is analyzed independently. This gives more information to a designer when choosing an optimal loop pairing.

$$\mathbf{c}_1 = \left[C^{c1}_{h_1,\hat{u}_1}, C^{c1}_{h_2,\hat{u}_2}, C^{c1}_{h_3,\hat{u}_3}, C^{c1}_{h_4,\hat{u}_4}\right] \tag{75}$$

$$\begin{bmatrix} v_1 \\ v_2 \\ \gamma_1 \\ \gamma_2 \end{bmatrix} = \begin{bmatrix} 0 & 0 & 0 & 1 \\ 0 & 0 & 1 & 0 \\ 1 & 0 & 0 & 0 \\ 0 & 1 & 0 & 0 \end{bmatrix} \begin{bmatrix} \hat{u}_1 \\ \hat{u}_2 \\ \hat{u}_3 \\ \hat{u}_4 \end{bmatrix} \tag{76}$$

$$C^{c1}_{h_1,\hat{u}_1} = \frac{K^{c1}_1(s+1/Ti^{c1}_1)}{s}, \quad C^{c1}_{h_2,\hat{u}_2} = \frac{K^{c1}_2(s+1/Ti^{c1}_2)}{s}$$
$$C^{c1}_{h_3,\hat{u}_3} = \frac{K^{c1}_3(s+1/Ti^{c1}_3)}{s}, \quad C^{c1}_{h_4,\hat{u}_4} = \frac{K^{c1}_4(s+1/Ti^{c1}_4)}{s} \tag{77}$$

$$\mathbf{x}^{c1} = \left[K^{c1}_1, Ti^{c1}_1, K^{c1}_2, Ti^{c1}_2, K^{c1}_3, Ti^{c1}_3, K^{c1}_4, Ti^{c1}_4\right] \tag{78}$$

$$\mathbf{c}_2 = \left[C^{c2}_{h_1,\hat{u}_1}, C^{c2}_{h_2,\hat{u}_2}, C^{c2}_{h_3,\hat{u}_3}, C^{c2}_{h_4,\hat{u}_4}\right] \tag{79}$$

$$\begin{bmatrix} v_1 \\ v_2 \\ \gamma_1 \\ \gamma_2 \end{bmatrix} = \begin{bmatrix} 1 & 0 & 0 & 0 \\ 0 & 1 & 0 & 0 \\ 0 & 0 & 0 & 1 \\ 0 & 0 & 1 & 0 \end{bmatrix} \begin{bmatrix} \hat{u}_1 \\ \hat{u}_2 \\ \hat{u}_3 \\ \hat{u}_4 \end{bmatrix} \tag{80}$$

$$C^{c2}_{h_1,\hat{u}_1} = \frac{K^{c2}_1(s+1/Ti^{c2}_1)}{s}, \quad C^{c2}_{h_2,\hat{u}_2} = \frac{K^{c2}_2(s+1/Ti^{c2}_2)}{s}$$
$$C^{c2}_{h_3,\hat{u}_3} = \frac{K^{c2}_3(s+1/Ti^{c2}_3)}{s}, \quad C^{c2}_{h_4,\hat{u}_4} = \frac{K^{c2}_4(s+1/Ti^{c2}_4)}{s} \tag{81}$$

$$\mathbf{x}^{c2} = \left[K^{c2}_1, Ti^{c2}_1, K^{c2}_2, Ti^{c2}_2, K^{c2}_3, Ti^{c2}_3, K^{c2}_4, Ti^{c2}_4\right] \tag{82}$$

$$\min_{\mathbf{x}^{ck}} \mathbf{J}(\mathbf{x}^{ck}) \tag{83}$$

$$\mathbf{J}(\mathbf{x}^{ck}) = \{J_1(\mathbf{x}^{ck}), J_2(\mathbf{x}^{ck}), J_3(\mathbf{x}^{ck}), J_4(\mathbf{x}^{ck}), J_5(\mathbf{x}^{ck}), J_6(\mathbf{x}^{ck}), J_7(\mathbf{x}^{ck}), J_8(\mathbf{x}^{ck})\} \tag{84}$$

$$\begin{aligned} J_\eta(\mathbf{x}^{ck}) = &\int_0^{t_f} |e_\eta|\Big|^{(h_2,h_3,h_4)=(h^0_2,h^0_3,h^0_4)}_{h_1=h^0_1+1cm} dt \\ &+ \int_0^{t_f} |e_\eta|\Big|^{(h_1,h_3,h_4)=(h^0_1,h^0_3,h^0_4)}_{h_2=h^0_2+1cm} dt \\ &+ \int_0^{t_f} |e_\eta|\Big|^{(h_1,h_2,h_4)=(h^0_1,h^0_2,h^0_4)}_{h_3=h^0_3+1cm} dt \\ &+ \int_0^{t_f} |e_\eta|\Big|^{(h_1,h_2,h_3)=(h^0_1,h^0_2,h^0_3)}_{h_4=h^0_4+1cm} dt \end{aligned} \tag{85}$$

$$\begin{aligned} J_{\eta+4}(\mathbf{x}^{ck}) = &\int_0^{t_f} \left|\frac{du_\eta}{dt}\right|\Big|^{(h_2,h_3,h_4)=(h^0_2,h^0_3,h^0_4)}_{h_1=h^0_1+1cm} dt \\ &+ \int_0^{t_f} \left|\frac{du_\eta}{dt}\right|\Big|^{(h_1,h_3,h_4)=(h^0_1,h^0_3,h^0_4)}_{h_2=h^0_2+1cm} dt \\ &+ \int_0^{t_f} \left|\frac{du_\eta}{dt}\right|\Big|^{(h_1,h_2,h_4)=(h^0_1,h^0_2,h^0_4)}_{h_3=h^0_3+1cm} dt \\ &+ \int_0^{t_f} \left|\frac{du_\eta}{dt}\right|\Big|^{(h_1,h_2,h_3)=(h^0_1,h^0_2,h^0_3)}_{h_4=h^0_4+1cm} dt \end{aligned} \tag{86}$$

$$\eta = 1 \textit{ to } 4$$
$$t_f = 1000 \textit{ seconds}$$

$$\underline{\mathbf{x}}^{ck} \leq \mathbf{x}^{ck} \leq \overline{\mathbf{x}}^{ck} \tag{87}$$

$$J_1(\mathbf{x}^{ck}) \leq 8000, \quad J_2(\mathbf{x}^{ck}) \leq 10000, \; J_3(\mathbf{x}^{ck}) \leq 2000,$$
$$J_4(\mathbf{x}^{ck}) \leq 5000, \quad J_5(\mathbf{x}^{ck}) \leq 3, \; J_6(\mathbf{x}^{ck}) \leq 3,$$
$$J_7(\mathbf{x}^{ck}) \leq 1, \quad J_8(\mathbf{x}^{ck}) \leq 1 \tag{88}$$

$$\mathbf{x}^{ck} = \left[K^{ck}_1, Ti^{ck}_1, K^{ck}_2, Ti^{ck}_2, K^{ck}_3, Ti^{ck}_3, K^{ck}_4, Ti^{ck}_4\right] \tag{89}$$

The bounds of $\mathbf{x}^{ck}$ are shown in the Table 11.

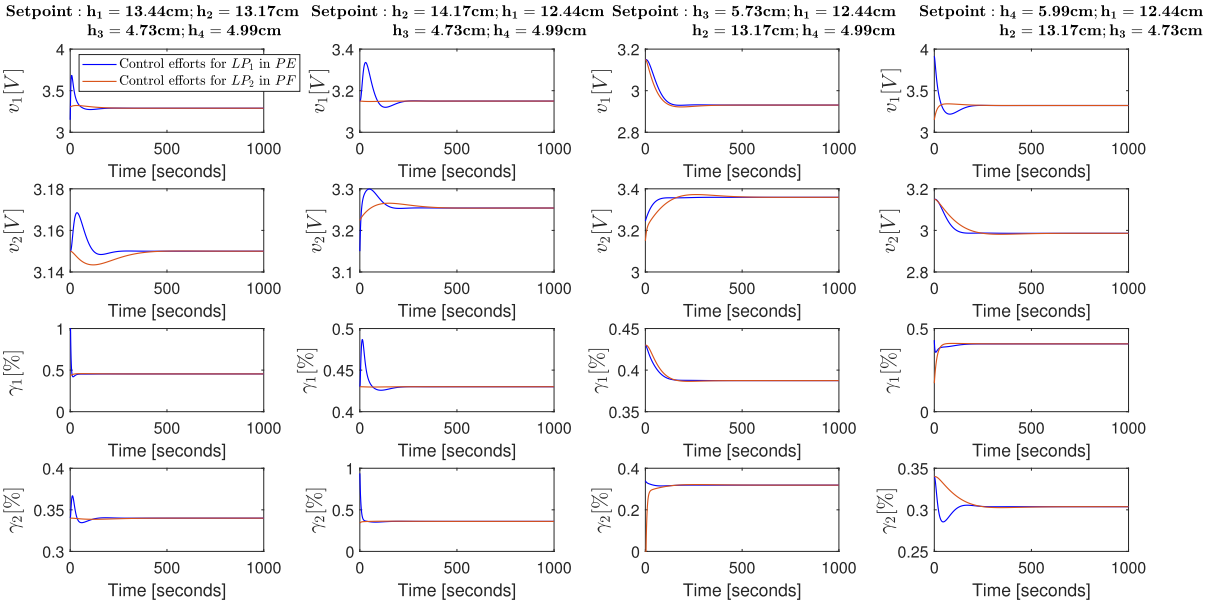

FIGURE 19. Control efforts of the controllers in *PE* and *PF*.

TABLE 10. PI diagonal and off-diagonal controllers selected in Fig. 16 [49] represents the controller proposed by Johansson.

PI off-diagonal controller		PI diagonal controller		
Parameters	*PD*	*Parameters*	*PC*	[49]
K_1^{c2}	0.313	K_1^{c1}	1.513	1.5
Ti_1^{c2}	78.02	Ti_1^{c1}	18.22	110
K_2^{c2}	0.289	K_2^{c1}	-0.086	-0.12
Ti_2^{c2}	133.62	Ti_2^{c1}	138.12	220
$J_1(\mathbf{x}^{c2})$	335.32	$J_1(\mathbf{x}^{c1})$	**48.94**	142.49
$J_2(\mathbf{x}^{c2})$	**514.25**	$J_2(\mathbf{x}^{c1})$	1685	1887.02
$J_3(\mathbf{x}^{c2})$	**0.609**	$J_3(\mathbf{x}^{c1})$	2.05	2.17
$J_4(\mathbf{x}^{c2})$	0.576	$J_4(\mathbf{x}^{c1})$	**0.452**	0.55

TABLE 11. Bounds of the decision vectors $\mathbf{x^{c1}}$ and $\mathbf{x^{c2}}$ for the third example.

Bounds of $\mathbf{x}^{ck}$								
$\mathbf{x}^{c1}$	K_1^{c1}	Ti_1^{c1}	K_2^{c1}	Ti_2^{c1}	K_3^{c1}	Ti_3^{c1}	K_4^{c1}	Ti_4^{c1}
$\underline{\mathbf{x}}^{c1}$	0.1	10	0.1	10	0.1	10	0.1	10
$\overline{\mathbf{x}}^{c1}$	1	50	1	30	1	50	1	100
x^{c2}	K_1^{c2}	Ti_1^{c2}	K_2^{c2}	Ti_2^{c2}	K_3^{c2}	Ti_3^{c2}	K_4^{c2}	Ti_4^{c2}
$\underline{\mathbf{x}}^{c2}$	0.1	10	0.1	10	-1	10	-1	10
$\overline{\mathbf{x}}^{c2}$	2	100	2	100	-0.1	100	-0.1	50

In the multi-objective optimization (MOO) stage of each MOP, the Pareto fronts shown in Fig. 17 were obtained. It is possible to visualize that the design concept $\mathbf{c}_1$ (loop pairing LP_1) has a better performance for the reference tracking of h_1 and h_2 than the design concept $\mathbf{c}_2$ (loop pairing LP_2), while the opposite is true for levels h_3 and h_4.

To analyze the trade-off between the IAE and IADU, a solution of each design concept (*PE* and *PF*) was selected, taking into consideration the regions with the best performances for h_1 and h_2, and also h_3 and h_4. The responses of the controllers in *PE* and *PF* are shown in Fig. 18.

TABLE 12. PIs controllers selected in Fig. 17.

PI-LP_2 controller		PI-LP_1 controller	
Parameters	*PF*	*Parameters*	*PE*
K_1^{c2}	0.152	K_1^{c1}	0.764
Ti_1^{c2}	51.95	Ti_1^{c1}	31.14
K_2^{c2}	0.074	K_2^{c1}	0.095
Ti_2^{c2}	57.39	Ti_2^{c1}	24.13
K_3^{c2}	-0.259	K_3^{c1}	0.884
Ti_3^{c2}	88.78	Ti_3^{c1}	26.29
K_4^{c2}	-0.579	K_4^{c1}	0.599
Ti_4^{c2}	24.32	Ti_4^{c1}	40.39
$J_1(\mathbf{x}^{c2})$	387.79	$J_1(\mathbf{x}^{c1})$	**17.50**
$J_2(\mathbf{x}^{c2})$	818.82	$J_2(\mathbf{x}^{c1})$	**28.58**
$J_3(\mathbf{x}^{c2})$	**20.25**	$J_3(\mathbf{x}^{c1})$	293.84
$J_4(\mathbf{x}^{c2})$	**75.08**	$J_4(\mathbf{x}^{c1})$	107.39
$J_5(\mathbf{x}^{c2})$	**0.505**	$J_5(\mathbf{x}^{c1})$	2.42
$J_6(\mathbf{x}^{c2})$	**0.476**	$J_6(\mathbf{x}^{c1})$	0.518
$J_7(\mathbf{x}^{c2})$	**0.319**	$J_7(\mathbf{x}^{c1})$	0.904
$J_8(\mathbf{x}^{c2})$	**0.391**	$J_8(\mathbf{x}^{c1})$	0.768

The controller in *PE* has a better performance than the controller in *PF* for reference tracking at levels h_1 and h_2 as shown in Fig. 18 and in objectives $J_1(\mathbf{x}^{c1})$ and $J_2(\mathbf{x}^{c1})$ shown in Table 12. For reference tracking at levels h_3 and h_4, the controller in *PF* has a better performance than the controller in *PE* as shown in Fig. 18 and in the objectives $J_3(\mathbf{x}^{c2})$ and $J_4(\mathbf{x}^{c2})$ shown in Table 12. With respect to control efforts, the controller in *PF* is less aggressive than the controller in *PE* as shown in Fig. 19, and in objectives $J_5(\mathbf{x}^{c2})$, $J_6(\mathbf{x}^{c2})$, $J_7(\mathbf{x}^{c2})$, $J_8(\mathbf{x}^{c2})$ as shown in Table 12.

VII. CONCLUSION

This paper shows a new framework for analyzing the problem of selecting optimal input-output pairings for decentralized control of non-linear multivariable systems. The proposal

presented in this paper follows a multi-objective optimization approach by extending the methodology shown in [46] for application in non-linear multivariable systems.

An interesting aspect of the proposed methodology is that the optimal tuning of each controller and the loop pairing are embedded in the multi-objective optimization process. By simulating the closed loop system, the proposed technique enables analyzing the characteristics of the system for a designer to make a decision according to his or her preferences. This aspect logically increases the computational cost of the technique, but it has the advantage that it enables analyzing in greater detail the problem of finding optimal loop pairings to efficiently control a multivariable non-linear system.

Three examples of application of the proposed methodology are shown. In these examples, the strong relationship between a designer's preferences and the selection of an optimal loop pairing has been demonstrated. The scenario contemplated in the problem statement (the operating point where the plant is operated and the structure of the controllers and design objectives) conditions the performance of each loop pairing. When a loop pairing is not clearly better than others, the proposed multi-objective methodology offers the control engineer a multi-dimensional approach to solve a loop pairing problem and make decisions with more information and based on preferences.

In the first example presented (coupled two-tank) it was shown that the application of the loop pairing technique to the linearized system can generate results that do not coincide with those obtained by applying the technique directly to the non-linear system. This gives more added value to the loop pairing techniques that can be applied directly to non-linear systems (such as the technique presented in this paper) than those techniques that need to linearize the plant before application.

In the second example (2×2 quadruple-tank system) the proposed methodology was applied directly to the non-linear system. It was found that there is a trade-off between the performances of each loop pairing. This trade-off between loop pairings means that one of the input-output pairings is better for controlling one of the outputs and vice versa. This shows that no loop pairing is better than another in all aspects and that a designer could choose one or the other depending on his/her preferences.

The third example is aimed at showing the scalability of the methodology. In this case, it was applied to the same non-linear system of the second example, but increasing its order (4×4 quadruple-tank system). In this example, there is one loop pairing that is better for controlling two of the system outputs (levels h_1 and h_2) and the other loop pairing is better for controlling the other two outputs (levels h_3 and h_4). This shows that there is a trade-off between the input-output pairings. It is worth noticing that, in this example, thanks to the methodology proposed, not only an optimal loop pairing (according to the designer's preferences) was found but also the control parameter tuning was carried out at the same time, a tuning, moreover, that outperforms the ones proposed in [49].

Future work will focus on expanding the methodology proposed in this paper for application in uncertain multivariable systems since traditional loop pairing techniques cannot analyze this effect and it can degrade the efficiency of decentralized control.

As a final comment, it is worth mentioning that it will be necessary 1) to improve the optimization algorithms in order to face the increasing complexity of controlling MIMO systems of many variables and 2) to consider the possibility of incorporating more indicators in the multi-objective problem. In other words, for the methodology proposed in this paper to be applicable to a higher scale, it is necessary to achieve computational improvements in the optimization algorithms.

REFERENCES

[1] L. Bakule, "Decentralized control: Status and outlook," *Annu. Rev. Control*, vol. 38, no. 1, pp. 71–80, Jan. 2014.

[2] L. A. Amezquita-Brooks, J. Liceaga-Castro, E. Liceaga-Castro, and C. E. Ugalde-Loo, "Induction motor control: Multivariable analysis and effective decentralized control of stator currents for high-performance applications," *IEEE Trans. Ind. Electron.*, vol. 62, no. 11, pp. 6818–6832, Nov. 2015.

[3] H. Sun, G. Zong, and C. L. P. Chen, "Adaptive decentralized output feedback PI tracking control design for uncertain interconnected nonlinear systems with input quantization," *Inf. Sci.*, vol. 512, pp. 186–206, Feb. 2020.

[4] F. Wallam and C. P. Tan, "Output feedback cross-coupled nonlinear PID based MIMO control scheme for pressurized heavy water reactor," *J. Franklin Inst.*, vol. 356, no. 15, pp. 8012–8048, Oct. 2019.

[5] E. F. Camacho and C. Bordons, *Model Predictive Control*, vol. 2. London, U.K.: Springer-Verlag, 2007.

[6] K. M. Abughalieh and S. G. Alawneh, "A survey of parallel implementations for model predictive control," *IEEE Access*, vol. 7, pp. 34348–34360, 2019.

[7] E. Bristol, "On a new measure of interaction for multivariable process control," *IEEE Trans. Autom. Control*, vol. 11, no. 1, pp. 133–134, Jan. 1966.

[8] X. Luo, P. Cao, and F. Xu, "Dynamic interaction analysis and pairing evaluation in control configuration design," *Chin. J. Chem. Eng.*, vol. 24, no. 7, pp. 861–868, Jul. 2016.

[9] L. Lenis, M. A. Giraldo, and J. J. Espinosa, "Methodology for the decomposition of dynamical systems based on input-output pairing techniques," in *Proc. IEEE 3rd Colombian Conf. Autom. Control (CCAC)*, Oct. 2017, pp. 1–7.

[10] B. Moaveni and W. Birk, "Modified hankel interaction index array for input-output pairing with improved characteristics," *IFAC-PapersOnLine*, vol. 51, no. 18, pp. 452–457, 2018.

[11] A. S. Potts, C. S. Morales Alvarado, and C. Garcia, "Input-output pairs detection in a distillation column operating in closed-loop," *IFAC-PapersOnLine*, vol. 51, no. 10, pp. 205–210, 2018.

[12] P. Daoutidis and C. Kravaris, "Structural evaluation of control configurations for multivariable nonlinear processes," *Chem. Eng. Sci.*, vol. 47, no. 5, pp. 1091–1107, Apr. 1992.

[13] S. T. Glad, "Extensions of the RGA concept to nonlinear systems," in *Proc. Eur. Control Conf. (ECC)*, Aug. 1999, pp. 961–963.

[14] B. Moaveni and A. Khaki-Sedigh, "Input-output pairing for nonlinear multivariable systems," *J. Appl. Sci.*, vol. 7, no. 22, pp. 3492–3498, Dec. 2007.

[15] A. Khaki-Sedigh and B. Moaveni, *Control Configuration Selection for Multivariable Plants*, vol. 391. Berlin, Germany: Springer-Verlag, 2009.

[16] Y. Zhang, S. Li, and L. Liao, "Near-optimal control of nonlinear dynamical systems: A brief survey," *Annu. Rev. Control*, vol. 47, pp. 71–80, Feb. 2019.

[17] M. Mavrovouniotis, C. Li, and S. Yang, "A survey of swarm intelligence for dynamic optimization: Algorithms and applications," *Swarm Evol. Comput.*, vol. 33, pp. 1–17, Apr. 2017.

[18] O. Ertenlice and C. B. Kalayci, "A survey of swarm intelligence for portfolio optimization: Algorithms and applications," *Swarm Evol. Comput.*, vol. 39, pp. 36–52, Apr. 2018.
[19] Z. Wang and A. Sobey, "A comparative review between genetic algorithm use in composite optimisation and the state-of-the-art in evolutionary computation," *Composite Struct.*, vol. 233, Feb. 2020, Art. no. 111739.
[20] I. Strumberger, E. Tuba, N. Bacanin, R. Jovanovic, and M. Tuba, "Convolutional neural network architecture design by the tree growth algorithm framework," in *Proc. Int. Joint Conf. Neural Netw. (IJCNN)*, Jul. 2019, pp. 1–8.
[21] I. Strumberger, E. Tuba, N. Bacanin, M. Zivkovic, M. Beko, and M. Tuba, "Designing convolutional neural network architecture by the firefly algorithm," in *Proc. Int. Young Eng. Forum (YEF-ECE)*, May 2019, pp. 59–65.
[22] K. M. Sagayam and D. J. Hemanth, "ABC algorithm based optimization of 1-D hidden Markov model for hand gesture recognition applications," *Comput. Ind.*, vol. 99, pp. 313–323, Aug. 2018.
[23] M. G. H. Omran and S. Al-Sharhan, "Improved continuous ant colony optimization algorithms for real-world engineering optimization problems," *Eng. Appl. Artif. Intell.*, vol. 85, pp. 818–829, Oct. 2019.
[24] A. Baykasoğlu, A. Hamzadayi, and S. Akpinar, "Single seekers society (SSS): Bringing together heuristic optimization algorithms for solving complex problems," *Knowl.-Based Syst.*, vol. 165, pp. 53–76, Feb. 2019.
[25] J. Wan, W. Liu, X. Ding, B. He, R. Nian, Y. Shen, and T. Yan, "Fractional order PID motion control based on seeker optimization algorithm for AUV," in *Proc. OCEANS MTS/IEEE Charleston*, Oct. 2018, pp. 1–4.
[26] B. Jamali, M. Rasekh, F. Jamadi, R. Gandomkar, and F. Makiabadi, "Using PSO-GA algorithm for training artificial neural network to forecast solar space heating system parameters," *Appl. Thermal Eng.*, vol. 147, pp. 647–660, Jan. 2019.
[27] H. Garg, "A hybrid PSO-GA algorithm for constrained optimization problems," *Appl. Math. Comput.*, vol. 274, pp. 292–305, Feb. 2016.
[28] J. O. Hernández-Vázquez, S. Hernández-González, J. A. Jiménez-García, M. D. Hernández-Ripalda, and J. I. Hernández-Vázquez, "Hybrid metaheuristic approach GA-SA for the buffer allocation problem that minimizes the work in process in open serial production lines," *Revista Iberoamericana Automatica Inform. Ind.*, vol. 16, no. 4, pp. 447–448, 2019.
[29] G. R. Meza, X. Blasco, J. Sanchis, and J. M. Herrero, *Controller Tuning With Evolutionary Multiobjective Optimization: A Holistic Multiobjective Optimization Design Procedure*, vol. 85. Cham, Switzerland: Springer, 2016.
[30] W. Boukadida, A. Benamor, H. Messaoud, and P. Siarry, "Multi-objective design of optimal higher order sliding mode control for robust tracking of 2-DoF helicopter system based on metaheuristics," *Aerosp. Sci. Technol.*, vol. 91, pp. 442–455, Aug. 2019.
[31] V. Huilcapi, B. Lima, X. Blasco, and J. M. Herrero, "Multi-objective optimization in modeling and control for rotary inverted pendulum," *Revista Iberoamericana Automatica Inform. Ind.*, vol. 15, no. 4, pp. 363–373, 2018.
[32] M. G. Villarreal-Cervantes, A. Rodriguez-Molina, C.-V. Garcia-Mendoza, O. Penaloza-Mejia, and G. Sepulveda-Cervantes, "Multi-objective on-line optimization approach for the DC motor controller tuning using differential evolution," *IEEE Access*, vol. 5, pp. 20393–20407, 2017.
[33] X. Zhou, J. Zhou, C. Yang, and W. Gui, "Set-point tracking and multi-objective optimization-based PID control for the goethite process," *IEEE Access*, vol. 6, pp. 36683–36698, 2018.
[34] M. Behzadian, S. Khanmohammadi Otaghsara, M. Yazdani, and J. Ignatius, "A state-of the-art survey of TOPSIS applications," *Expert Syst. Appl.*, vol. 39, no. 17, pp. 13051–13069, Dec. 2012.
[35] J. Zhu and K. W. Hipel, "Multiple stages grey target decision making method with incomplete weight based on multi-granularity linguistic label," *Inf. Sci.*, vol. 212, pp. 15–32, Dec. 2012.
[36] B. Nasseh Chaffi and F. Soltani Tafreshi, "Nasseh method to visualize high-dimensional data," *Appl. Soft Comput.*, vol. 84, Nov. 2019, Art. no. 105722.
[37] W. J. Raseman, J. Jacobson, and J. R. Kasprzyk, "Parasol: An open source, interactive parallel coordinates library for multi-objective decision making," *Environ. Model. Softw.*, vol. 116, pp. 153–163, Jun. 2019.
[38] T. Tusar and B. Filipic, "Visualization of Pareto front approximations in evolutionary multiobjective optimization: A critical review and the prosection method," *IEEE Trans. Evol. Comput.*, vol. 19, no. 2, pp. 225–245, Apr. 2015.
[39] B. Filipič and T. Tušar, "A taxonomy of methods for visualizing Pareto front approximations," in *Proc. Genetic Evol. Comput. Conf. (GECCO)*, 2018, pp. 649–656.
[40] X. Blasco, G. Reynoso-Meza, E. A. Sánchez Pérez, and J. V. Sánchez Pérez, "Asymmetric distances to improve n -dimensional Pareto fronts graphical analysis," *Inf. Sci.*, vols. 340–341, pp. 228–249, May 2016.
[41] X. Blasco, J. M. Herrero, J. Sanchis, and M. Martínez, "A new graphical visualization of n-dimensional Pareto front for decision-making in multiobjective optimization," *Inf. Sci.*, vol. 178, no. 20, pp. 3908–3924, Oct. 2008.
[42] X. Blasco, J. M. Herrero, G. Reynoso-Meza, and M. A. M. Iranzo, "Interactive tool for analyzing multiobjective optimization results with level diagrams," in *Proc. Genetic Evol. Comput. Conf. Companion (GECCO)*, 2017, pp. 1689–1696.
[43] J. M. Herrero, X. Blasco, M. Martínez, C. Ramos, and J. Sanchis, "Nonlinear robust identification of a greenhouse model using multi-objective evolutionary algorithms," *Biosyst. Eng.*, vol. 98, no. 3, pp. 335–346, Nov. 2007.
[44] J. M. Herrero, J. M. Martínez, J. Sanchis, and X. Blasco, "Well-distributed Pareto front by using the evMOGA evolutionary algorithm," in *Proc. 9th Int. Work Conf. Artif. Neural Netw.*, Berlin, Germany: Springer-Verlag, 2007, p. 292–299.
[45] A. Susperregui, J. M. Herrero, M. I. Martinez, G. Tapia-Otaegui, and X. Blasco, "Multi-objective optimisation-based tuning of two second-order sliding-mode controller variants for DFIGs connected to non-ideal grid voltage," *Energies*, vol. 12, no. 19, p. 3782, Oct. 2019.
[46] V. Huilcapi, X. Blasco, J. M. Herrero, and G. Reynoso-Meza, "A loop pairing method for multivariable control systems under a multi-objective optimization approach," *IEEE Access*, vol. 7, pp. 81994–82014, 2019.
[47] J. M. Herrero, G. Reynoso-Meza, C. Ramos, and X. Blasco, "Considerations on loop pairing in MIMO processes. A multi-criteria analysis," *IFAC-PapersOnLine*, vol. 50, no. 1, pp. 4454–4459, 2017.
[48] H. Gouta, S. Hadj Saïd, A. Turki, and F. M'Sahli, "Experimental sensorless control for a coupled two-tank system using high gain adaptive observer and nonlinear generalized predictive strategy," *ISA Trans.*, vol. 87, pp. 187–199, Apr. 2019.
[49] K. H. Johansson, "The quadruple-tank process: A multivariable laboratory process with an adjustable zero," *IEEE Trans. Control Syst. Technol.*, vol. 8, no. 3, pp. 456–465, May 2000.
[50] G. Reynoso-Meza, X. Blasco, J. Sanchis, and J. M. Herrero, "Comparison of design concepts in multi-criteria decision-making using level diagrams," *Inf. Sci.*, vol. 221, pp. 124–141, Feb. 2013.
[51] M. Laszczyk and P. B. Myszkowski, "Survey of quality measures for multi-objective optimization: Construction of complementary set of multi-objective quality measures," *Swarm Evol. Comput.*, vol. 48, pp. 109–133, Aug. 2019.
[52] S. Rojas-Gonzalez and I. Van Nieuwenhuyse, "A survey on kriging-based infill algorithms for multiobjective simulation optimization," *Comput. Oper. Res.*, vol. 116, Apr. 2020, Art. no. 104869.
[53] Y. Xue, M. Li, M. Shepperd, S. Lauria, and X. Liu, "A novel aggregation-based dominance for Pareto-based evolutionary algorithms to configure software product lines," *Neurocomputing*, vol. 364, pp. 32–48, Oct. 2019.

VÍCTOR HUILCAPI received the degree in electronic engineering and the M.Sc. degree in automation and industrial control from the Escuela Superior Politécnica del Litoral (ESPOL), Guayaquil, Ecuador, in 2002 and 2015, respectively. He is currently pursuing the Ph.D. degree with the Universitat Politècnica de València (UPV), Spain. He is also an Associate Lecturer with the Universidad Politécnica Salesiana (UPS). His main research interests are control and modeling of multivariable systems, process optimization, and multiobjective optimization techniques applied to engineering.

XAVIER BLASCO received the B.S. degree in industrial engineering from the Universitat Politècnica de València (UPV), Spain, in 1991, the Diplome de Spécialisation en Génie Electrique degree from the Ecole Supérieure d'Electricité (SUPELEC), France, in 1992, and the Ph.D. degree in industrial engineering from UPV, in 1999. Since 1994, he has been a Lecturer with the Department of Systems Engineering and Automation, UPV. He is currently a Full Professor. His research work is developed at the Institute of Automatic Control (ai2 - UPV). His research interests are model-based predictive control, evolutionary optimization and multiobjective optimization applied to engineering, and dynamic modeling and process control.

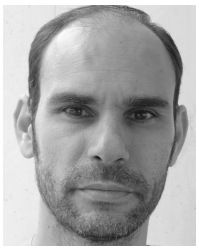

JUAN MANUEL HERRERO received the B.S. and Ph.D. degrees in control systems engineering from the Universitat Politècnica de València (UPV), in 1999 and 2006, respectively. He is currently an Associate Lecturer with the Department of Systems Engineering and Automation, UPV. His main research interests are multivariable predictive control, process optimization, and computational intelligence methods for control engineering.

GILBERTO REYNOSO-MEZA received the B.Sc. degree in mechanical engineering from the Tecnológico de Monterrey, Campus Querétaro, Mexico, in 2001, and the Ph.D. degree in automation from the Universitat Politècnica de València, Spain. He is currently an Associate Professor with the Industrial and Systems Engineering Graduate Program (PPGEPS), Pontifical Catholic University of Parana (PUCPR), Brazil. His main research interests are computational intelligence methods for control engineering and design, multiobjective optimization, many-objectives optimization, multicriteria decision making, evolutionary algorithms, and machine learning.